DANMARKS OG GRØNLANDS GEOLOGISKE UNDERSØGELSE RAPPORT 2010/10

Geological, petrographical and lithogeochemical investigations on the Qussuk gold mineralisation, southern West Greenland

Denis Martin Schlatter & Rasmus Christensen

GEOLOGICAL SURVEY OF DENMARK AND GREENLAND
MINISTRY OF CLIMATE AND ENERGY

GEUS

DANMARKS OG GRØNLANDS GEOLOGISKE UNDERSØGELSE RAPPORT 2010/10

Geological, petrographical and lithogeochemical investigations on the Qussuk gold mineralisation, southern West Greenland

Denis Martin Schlatter & Rasmus Christensen

GEOLOGICAL SURVEY OF DENMARK AND GREENLAND
MINISTRY OF CLIMATE AND ENERGY

GEUS

Contents

Abstract

Gold exploration in the Nuuk area has only been carried out since the early 1990's. However, the Godthåbsfjord is now recognised as a gold province with several projects being brought to drilling stage. Qussuk is located about 70 km NNE of Nuuk in the Akia terrane of the North Atlantic craton. The SW-NE trending Ivinnguit fault separates the Akia terrane in the north from the Færingehavn terrane in the south, and is the locus of several hydrothermal gold occurrences. These are from north to south: Isua, Qussuk, Storø, Bjørneø and Qilanngaarsuit.

The Qussuk prospect is about 20 km long, 2 to 3 km wide, and is divided from north to south into the Swan N, the Swan and the Plateau areas. The rocks at Qussuk are metamorphosed to amphibolite facies grade. They comprise amphibolite, meta-ultramafic rocks, and aluminous and tonalitic gneiss. Deformation is characterised by isoclinal folds, which are upright to overturned; the foliation trends NNE-SSW and is near vertical.

In the Swan N area, a 120 m thick rock sequence consists of up to 30 m thick leuco-amphibolite, up to 10 m thick amphibolite, up to 25 m thick aluminous gneiss, up to 10 m thick biotite schist and 0.5 m to 5 m thick pegmatite dykes. At the contact of the aluminous gneiss and the leuco-amphibolite, a 23 m thick zone consists mainly of biotite schist with 5 cm to 30 cm thick quartz veins and quartz blebs. This zone is interpreted as the alteration zone and contains quartz, biotite, muscovite, sulphides, garnet and sillimanite. Gold content is 1.24 ppm Au over 23 m and a shorter section within this zone contains 8.4 ppm Au over 2 m.

In the Plateau area, a 100 m thick sequence comprises up to 40 m thick amphibolite, up to 10 m thick aluminous gneiss, up to several meter thick biotite schist, about 1 m thick leuco-amphibolite and 0.5 m to 5 m wide pegmatite dykes. At or close to the contact of amphibolite and leuco-amphibolite, several up to 0.5 m thick quartz veins occur. One of these quartz veins contains visible gold and is flanked by 0.5 m thick zones of inner semi-massive to massive pyrrhotite and outer biotite-quartz alteration. Analyses of this zone yield up to 19 ppm gold over 0.6 m.

The rock sequences of Plateau and Swan N are different and no straight forward geological correlation between the two areas can be made. However, the zones enriched in gold occur in both areas close to lithological contacts.

In the Swan area, no intersection with gold above 1 ppm was encountered.

Application of immobile-element methods to 50 whole-rock analyses show that the rocks from Plateau, Swan N and Swan can be classified into 10 different chemical groups ranging from andesite to basalt, and that the rocks are mainly meta-basalts and meta-basaltic andesite with transitional to calc-alkaline affinity and only few are tholeiitic. The rocks of the Au-zones of Swan N and Plateau comprise mainly basaltic andesite I of a calc-alkaline affinity.

Hydrothermal alteration zones at Swan N and Plateau comprise biotite, muscovite, quartz, pyrrhotite and chalcopyrite and small gold-quartz veins which in turn are rimmed by biotite. The gold mineralisation comprises quartz veins with visible gold (VG) and massive or disseminated pyrrhotite. Garnet, epidote and quartz occur together with biotite in the distal alteration zone.

The hydrothermal fluids are interpreted to have been enriched in potassium, silica, iron and gold. Chlorite replacing biotite and amphibole replacing pyroxene are regarded as retrograde metamorphic minerals.

Although the alteration seen at Swan N and Plateau is similar in style, the alteration zone in Plateau is narrower (a few metres) than in Swan N (tens of metres).

In order to find more gold mineralised systems in the Qussuk area, rocks of basaltic andesite I should be identified. This basaltic andesite I rock is a potential target if the layer is enveloped by

proximal alteration (quartz veins, pyrrhotite, elevated gold) and distal alteration (biotite, muscovite, quartz, sulphides, elevated gold).

Key words
Silicification · biotite alteration · Au-zone · visible gold · quartz veins · chemical rock types · hydrothermal alteration · Ivinnguit fault · orogenic gold deposit · Akia terrane · Færingehavn terrane · North Atlantic craton · Archaean · Godthåbsfjord · southern West Greenland

Introduction

Gold exploration in the Nuuk area has only been carried out since the early 1990's. However, the Godthåbsfjord is now recognised as a gold province (Appel et al. 2005). Several gold targets of the Godthåbsfjord were drill tested by exploration companies. Storø, which is located about 45 km north-east of Nuuk (Fig. 1), is the most advanced exploration project for gold in the Nuuk area. At Storø extensive core drilling and bulk sampling has been recently carried out by NunaMinerals (Østergaard, 2007; NunaMinerals company information, 2008a, b and c).

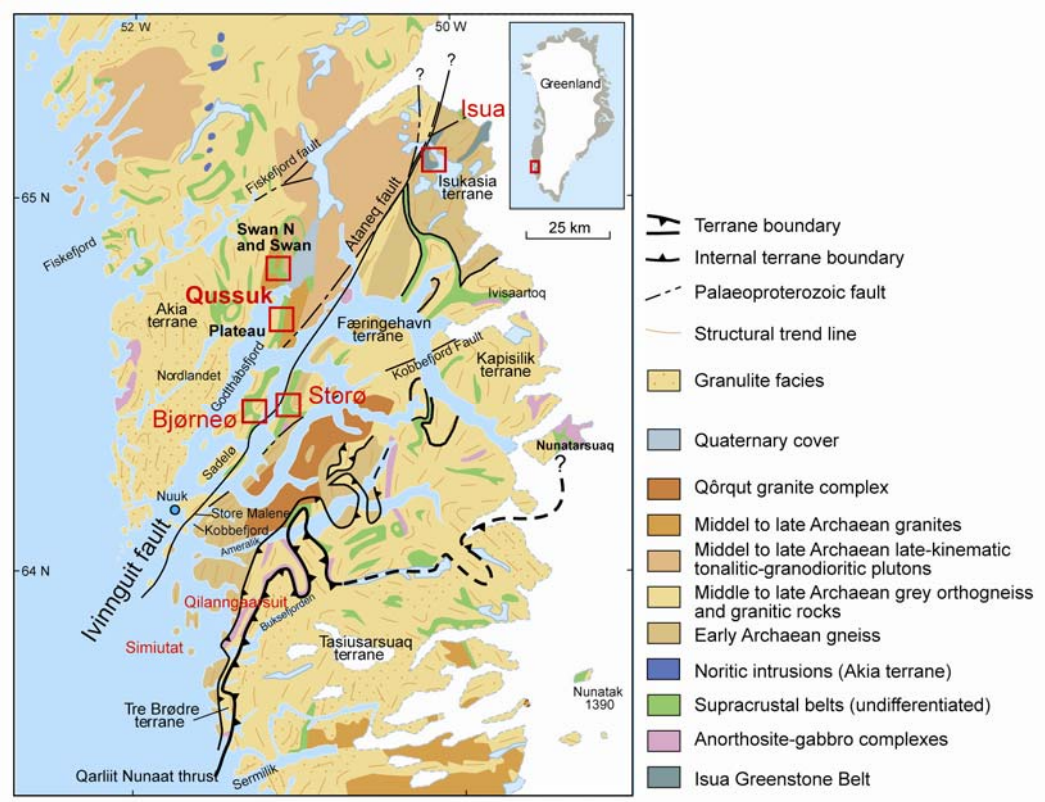

Figure 1. *Geology of the Nuuk area and gold occurrences of the Godthåbsfjord, modified from Escher and Pulvertaft, 1995. Qussuk is located about 70 km NNE of Nuuk and comprises the Swan N, Swan and Plateau areas.*

Qussuk is located about 70 km NNE of Nuuk in the Akia terrane of the North Atlantic craton (Fig. 1). The SW-NE trending Ivinnguit fault separates the 3200 Ma to 2975 Ma old Akia terrane in the north from the Færingehavn terrane in the south, and is the locus of several hydrothermal gold occurrences (Fig. 1). These Au-occurrences from north to south are: Isua, Qussuk, Storø, Bjørneø and Qilanngaarsuit (Fig. 1; Stensgaard 2008; Kolb et al. 2009). Interestingly several of these gold showings are spatially associated with base metal showings. An area located south of Qussuk known as Bjørneø (Fig. 1) hosts several small semi-massive to massive sulphide occurrences, which are elevated in Zn-Cu±Au±Pb±Ag and Au±Cu-Zn (Smith 1998). Another area where gold is found near base metal occurrences is located about 30 km south of Nuuk, in the Færingehavn terrane (Fig. 1). Here gold occurrences (without base metals) occur on Qilanngaarsuit and base-metal occurrences (without gold) occur on Simiutat, only a few kilometres apart (Kolb et al. 2009).

Figure 2 shows the most favourable areas to host gold occurrences as outlined by multiparameter spatial modelling by Stensgaard (2008: for location see figure 1). The outcome of the modelling clearly shows that areas which are spatially associated with the Ivinnguit and the Ataneq fault are most favourable to host gold.

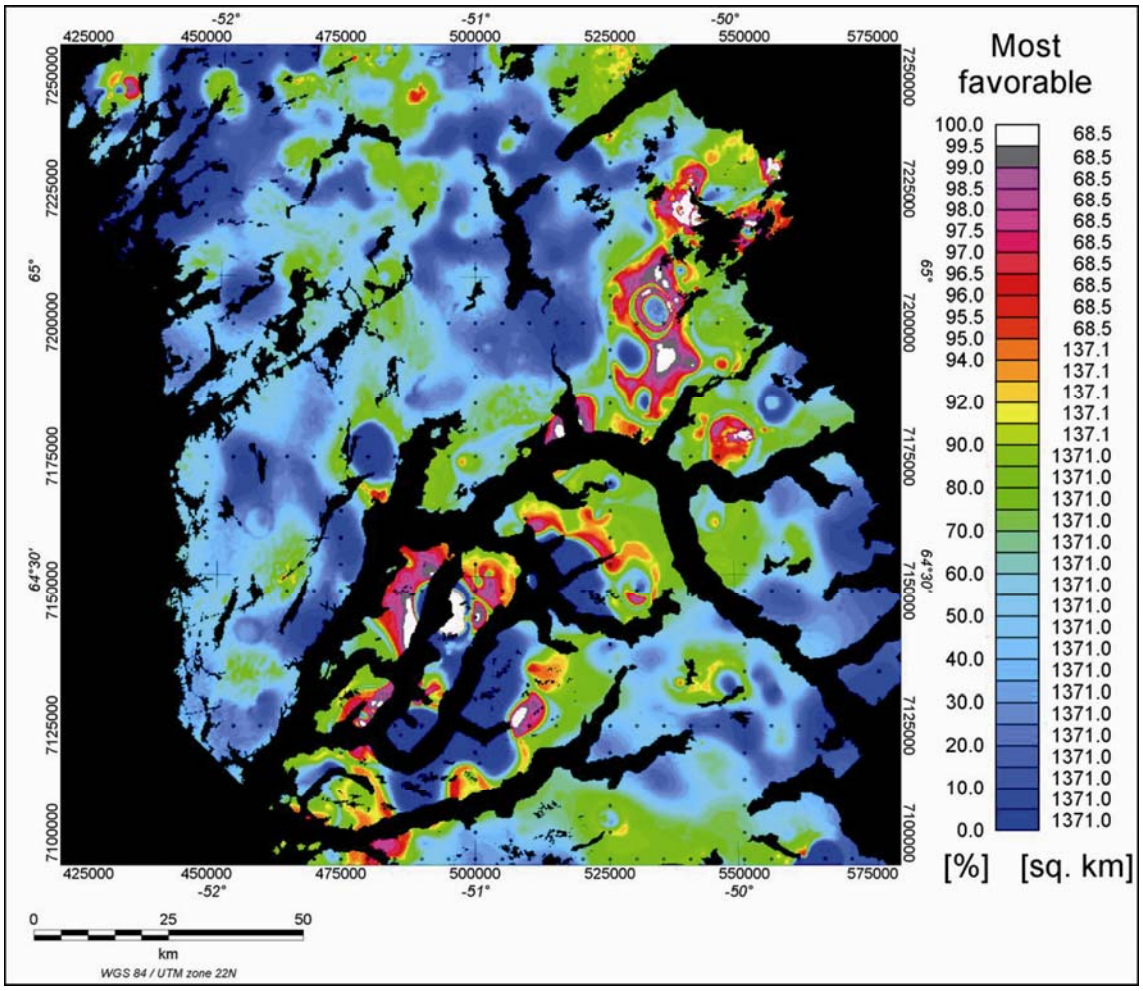

Figure 2. *Results of multiparameter spatial modeling of the Godthåbsfjord area (Stensgaard Møller 2008).*

NunaMinerals recently discovered gold anomalies in metamorphosed Archaean greenstones at Qussuk in south-West Greenland (Fig. 3a and b; Schlatter and Christensen 2010). The Qussuk area is located at the end of the Godthåbsfjord about 70 km NNE of Nuuk, covers 627 km^2 and is part of the NunaMinerals Storø concession license (Christensen 2007, 2008).

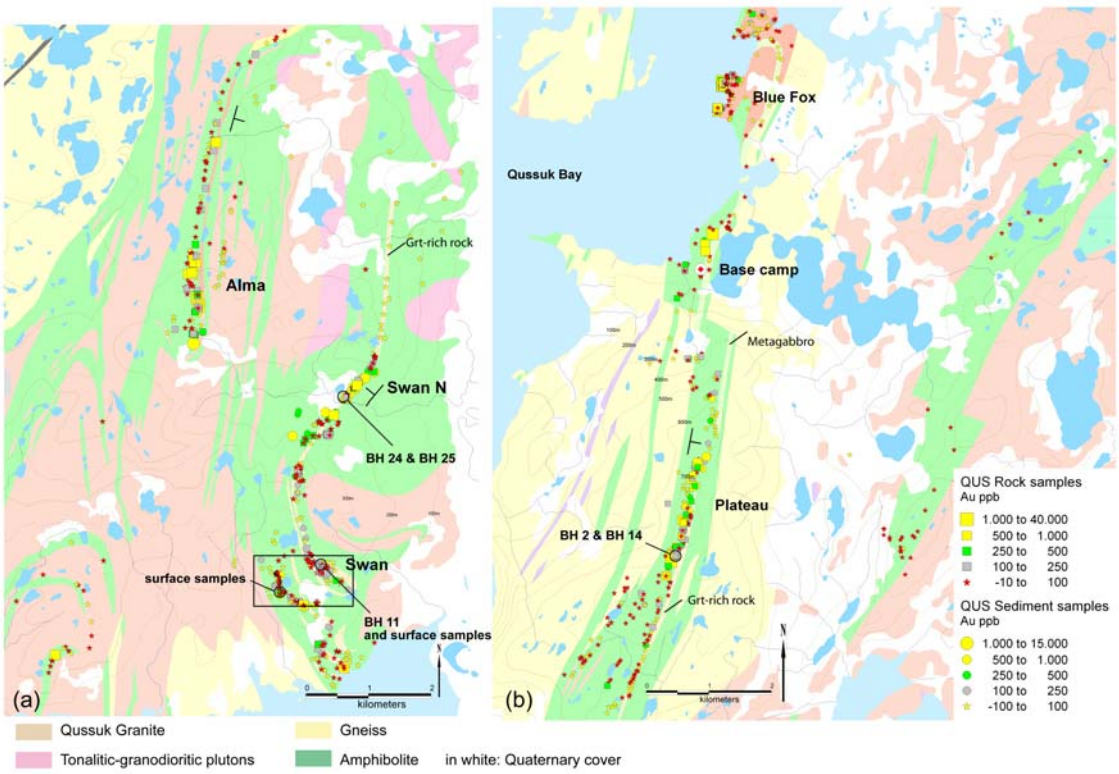

Figure 3. *Local Geology of the Qussuk area, modified from Garde, 1988. Figure 3a shows the northern part and figure 3b the southern part of Qussuk. Gold contents of rock and sediment samples as well as location of bore holes are superimposed.*

Prospecting efforts done by NunaMinerals in the field seasons 2006/07 identified rocks with 21.7 ppm gold over 1.5 m at Blue Fox, and a rock with visible gold and 35.8 ppm Au in the Plateau area (Fig. 3b; Christensen 2007 and 2008; NunaMinerals 2008a and b). Based on these and other promising results from the initial grass roots exploration, follow-up prospecting at surface was carried out and figures 3a and 3b show the results of surface sampling.

NunaMinerals defined four drill targets from north to south these are Alma, Swan N, Swan (Fig. 3a) and Plateau (Fig. 3b; Christensen 2010, in preparation). In detail, these targets were selected based on geological, geochemical and geophysical (SkyTEM helicopter-born) survey results and tested by diamond core drilling during the summers of 2008 and 2009. Figure 4 shows a digital elevation model of the Qussuk area and superimposed are the location of diamond drilling carried out in 2008 and 2009. From north to south the following holes were drilled: Alma area (1); Swan N area (17); Swan area (4); Plateau area (20). Table 1 lists all the bore holes from Qussuk with drill intersections above 0.5 ppm Au and appendix A lists the Au and base metal contents and pathfinder trace elements of the bore holes drilled by NunaMinerals during the summers of 2008 and 2009 (the approximate locations of the bore holes is shown in figure 4). Table 1 and appendix A show that the Swan N and the Plateau areas have a good potential to host an economic gold mineralisation and that the Alma area deserves follow up work, whereas at Swan drilling has not identified a gold potential because the best intersection yields only 0.78 ppm over 2 m.

Table 1. *Au intersections ≥0.5 ppm in the Qussuk bore holes.*

DDH ID	Area	year of drilling	SAMPLE ID	FROM	TO	SAMPLE LENGTH	Au (ppb)	Ag (ppm)	Cu (ppm)	Zn (ppm)	Pb (ppm)	S (%	Mn (ppm)	As (ppm)	Mo (ppm)	Bi (ppm)	Sb (ppm)	W (ppm)
QUS 09 DDH-39	Alma	2009	175805	18,00	20,00	2,00	1410	< 0.2	328	13	4	1,09	447	2	1	< 2	< 2	92
QUS 09 DDH-39	Alma	2009	175810	32,00	34,00	2,00	752	< 0.2	757	186	6	1,72	441	< 2	1	< 2	< 2	< 10
QUS-08 DDH-25	Swan N	2008	190453	65,00	67,00	2,00	8460	0,2	72	225	10	0,19	719	3	3	-2	-2	-10
QUS 09 DDH-30	Swan N	2009	175622	44,00	46,00	2,00	4560	< 0.2	203	109	2	0,44	484	< 2	< 1	< 2	< 2	< 10
QUS-08 DDH-25	Swan N	2008	190438	45,00	46,00	1,00	3590	3,3	2200	102	5	3,41	635	-2	2	2	-2	-10
QUS-08 DDH-25	Swan N	2008	190446	53,00	54,00	1,00	3340	0,2	303	32	2	1,4	324	-2	-1	3	-2	-10
QUS 09 DDH-28	Swan N	2009	175586	54,00	56,00	2,00	2950	< 0.2	71	171	5	0,15	685	2	3	< 2	< 2	< 10
QUS 09 DDH-37	Swan N	2009	175758	57,00	59,00	2,00	1710	< 0.2	371	75	6	0,78	388	< 2	1	< 2	< 2	< 10
QUS-08 DDH-25	Swan N	2008	190445	52,00	53,00	1,00	1210	-0,2	194	18	2	0,85	250	-2	-1	3	-2	-10
QUS-08 DDH-24	Swan N	2008	190401	48,00	50,00	2,00	1060	-0,2	225	8	-2	0,45	262	-2	-1	2	-2	-10
QUS 09 DDH-26	Swan N	2009	175537	90,00	92,00	2,00	1040	< 0.2	140	45	3	0,63	455	< 2	1	< 2	< 2	< 10
QUS 09 DDH-37	Swan N	2009	175762	65,00	66,75	1,75	1010	0,4	354	170	2	1,64	419	< 2	1	< 2	< 2	< 10
QUS-08 DDH-12	Swan N	2008	189853	134,00	136,00	2,00	985	-0,2	27	124	6	0,05	470	-2	-1	-2	-2	-10
QUS 09 DDH-29	Swan N	2009	175606	40,00	42,00	2,00	958	0,4	758	104	< 2	1,19	444	< 2	1	< 2	< 2	< 10
QUS 09 DDH-28	Swan N	2009	175590	62,00	64,00	2,00	890	< 0.2	227	183	10	0,56	865	< 2	1	< 2	< 2	22
QUS 09 DDH-37	Swan N	2009	175753	43,00	44,50	1,50	856	< 0.2	261	43	< 2	0,55	516	< 2	2	< 2	< 2	< 10
QUS 09 DDH-31	Swan N	2009	175647	43,00	45,00	2,00	816	< 0.2	307	261	4	0,41	696	< 2	1	< 2	< 2	< 10
QUS-08 DDH-25	Swan N	2008	190444	51,00	52,00	1,00	795	0,2	234	40	4	1,12	399	-2	-1	3	-2	-10
QUS-08 DDH-25	Swan N	2008	190443	50,00	51,00	1,00	716	0,3	569	14	3	0,58	329	-2	-1	3	-2	-10
QUS 09 DDH-33	Swan N	2009	175683	42,00	44,00	2,00	668	< 0.2	182	135	3	0,64	861	< 2	2	< 2	< 2	< 10
QUS-08 DDH-24	Swan N	2008	190397	43,00	44,00	1,00	648	-0,2	124	79	2	0,49	485	-2	-1	-2	-2	-10
QUS 09 DDH-38	Swan N	2009	175798	103,00	105,00	2,00	544	1,3	868	550	103	1,02	848	< 2	6	2	7	290
QUS 09 DDH-40	Swan	2009	175860	86,00	88,00	2,00	783	< 0.2	1780	49	2	0,57	291	2	2	< 2	< 2	< 10
QUS-08 DDH-01	Plateau	2008	189031	65,00	65,60	0,60	14500	1,3	1730	74	5	2,22	390	-2	1	-2	-2	-10
QUS-08 DDH-15	Plateau	2008	189978	32,80	34,00	1,20	6680	4,2	3380	148	11	3,81	729	-2	2	4	-2	-10
QUS-08 DDH-14	Plateau	2008	189941	36,60	37,70	1,10	6440	1,2	797	83	3	1,27	410	-2	-1	-2	-2	-10
QUS-08 DDH-03	Plateau	2008	189126	39,50	41,00	1,50	4200	2,3	474	166	3	2,05	1060	-2	5	2	-2	-10
QUS-08 DDH-02	Plateau	2008	189069	46,00	48,00	2,00	3160	0,3	320	100	3	1,16	585	2	1	-2	-2	-10
QUS-08 DDH-06	Plateau	2008	189363	93,00	95,20	2,20	1720	0,3	483	56	-2	1,61	512	-2	-1	-2	-2	-10
QUS-08 DDH-18	Plateau	2008	190077	6,00	8,00	2,00	996	-0,2	162	51	-2	0,25	596	-2	-1	-2	-2	-10
QUS-08 DDH-03	Plateau	2008	189158	105,00	107,00	2,00	741	-0,2	49	121	5	0,22	784	-2	4	-2	-2	-10
QUS-08 DDH-03	Plateau	2008	189123	34,00	36,00	2,00	596	-0,2	53	51	3	0,4	426	-2	1	-2	-2	-10
QUS-08 DDH-05	Plateau	2008	189293	92,00	94,00	2,00	574	-0,2	224	40	3	0,76	512	-2	-1	-2	-2	-10
QUS-08 DDH-14	Plateau	2008	189930	18,00	19,50	1,50	529	0,5	542	43	2	0,88	598	-2	1	-2	-2	-10
QUS-08 DDH-01	Plateau	2008	189016	34,00	36,00	2,00	506	-0,2	21	63	2	0,02	477	-2	3	-2	-2	-10

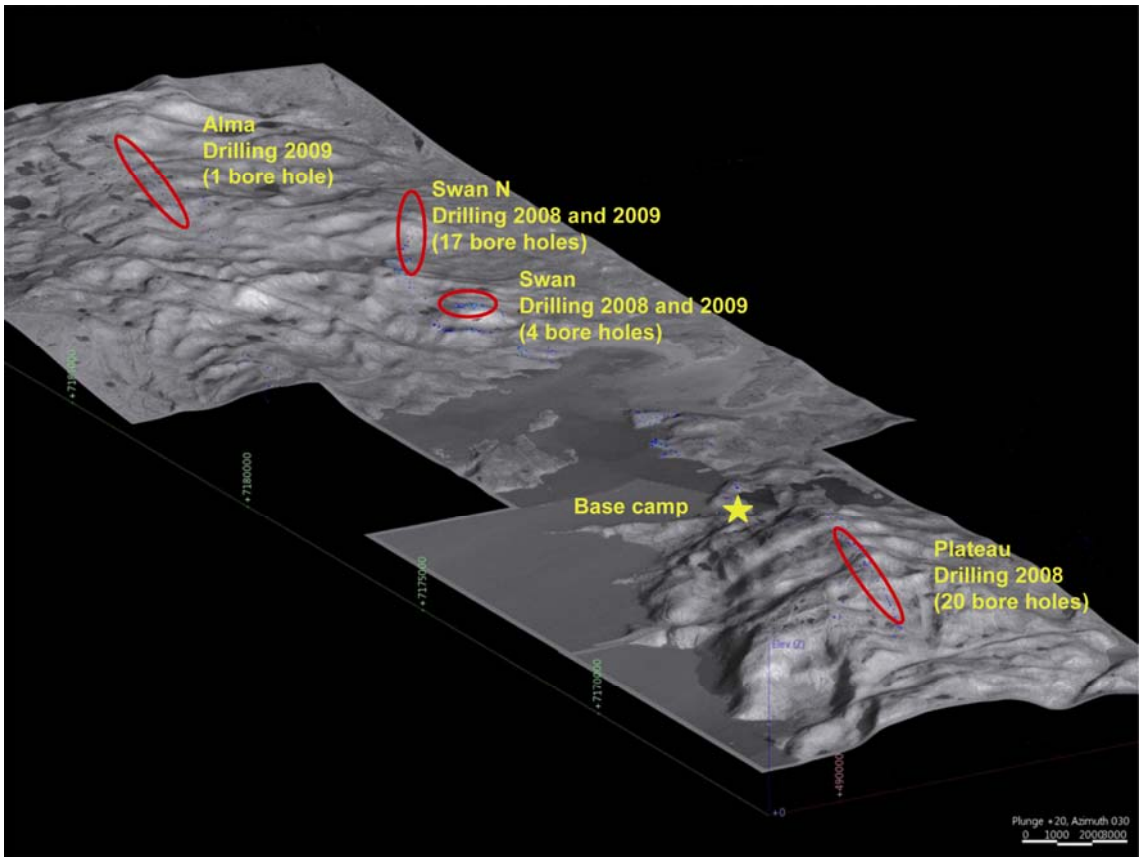

Figure 4. *Digital elevation model of the Qussuk area and location of drill programs 2008 and 2009. The small blue circles represent rock and sediment samples (for details see figure 3).*

Previous to drilling of the four Qussuk targets, the area has been thought to contain gold-copper mineralisation because of the occurrence of sulphides in the samples with elevated gold contents (Andreasen 2007). One rock immediately south of the Plateau area contains pyrite, chalcopyrite, covellite, pyrrhotite and goethite and yielded 8.16 ppm Au and 0.39 % Cu (Andreasen 2007). Another rock from the Blue Fox area contained pyrrhotite, chalcopyrite and marcasite and yielded 5.1 ppm Au and 0.11 % Cu (Andreasen 2007). Both samples yield less than 100 ppm in Zn and Pb and the Ag content is below 10 ppm (Andreasen 2007).
Drilling of 42 bore holes, of the four Qussuk targets shows that the only economic commodity is gold and that the samples with gold contents > 500 ppb generally have only low base metal contents, well below one percent of combined Cu+Pb+Zn (Table 1). Sulphur contents of these samples are also low and range between 0.02% and 3.9% and the Ag contents are between detection limit and 4.2 ppm.

Geology of the Qussuk area

The Qussuk area is located in the eastern most part of the Akia terrane (c. 3200 to 2975 Ma old), whereas the nearby Storø area is located in the Færingehavn terrane (c. 3600 to 2750 Ma old; Fig. 1). The two terranes are separated by the Ivinnguit fault (Hollis et al. 2004; 2005; 2006). The supracrustal rocks in the Qussuk area (Fig. 3) are metamorphosed to amphibolite grade, deformed and comprise amphibolite, ultramafic rocks, aluminous gneiss, tonalite and granite (Fig. 3; Garde 1997; Hollis et al. 2004). Deformation is characterised by isoclinal folds which are upright to overturned; the rocks are trending NNE-SSW and are steeply dipping (Garde 2008).

The age of the amphibolites in the Qussuk area is 3071 ± 1 Ma whereas tonalitic orthogneiss is 3060 to 3000 Ma old (U-Pb zircon age; Garde et al. 2007). These ages are supported by relative age relationships (Garde, in: Stendal 2007): The contact between orthogneiss and amphibolite was interpreted as intrusive with the tonalitic orthogneiss intruding into amphibolite. Plagioclase-rich amphibolites containing biotite and hornblende are possibly of pyroclastic or volcaniclastic origin as suggested by primary textures such as graded bedding, fragmental textures and presence of fiamme (Hollis et al. 2004; Garde 2007). The observation of these primary volcanic textures and the presence of calc-alkaline and tholeiitic andesites at Qussuk lead Garde (2008) to the conclusion that these rocks represent an Achaean island arc complex.

This study provides detailed geological descriptions from two drill profiles from the Swan N and from the Plateau area and reports the geochemical and petrological investigations from Swan N, Swan and Plateau. This study particularly aims at documenting in detail where gold mineralised units occur in the overall Qussuk lithology and at characterising the gold-rich units geologically, petrographically and geochemically. This study is directed towards helping gold-exploration to be more efficient in the Qussuk area, in the larger Nuuk area or elsewhere in the Achaean greenstone belts of southern West Greenland.

Methods

Field work was carried out in the Swan area, where 5 samples were taken from two surface profiles mainly for the lithogeochemical component of this study (Fig. 3; Appendix B).
The host rocks of the gold mineralisation were studied from drill cores from two sections (Appendix C; for details of the graphical logging technique used see McPhie et al. 1993).
In the Swan N and in Plateau area, two bore holes were studied, whereas one bore hole from the Swan area was studied in lesser detail. Figure 3 shows the location of the 5 bore holes which were investigated in this study (BH 2, 11, 14, 24 and 25). Drill core samples were about 20 to 25 cm long; and a quarter of the core was used for geochemical analyses. Drill core and rock samples were crushed by the Actlabs laboratory in Nuuk and analysed by the Actlabs laboratory in Ontario by Actlab's package "4Lithoresearch". Gold was analysed by instrumental neutron activation (INNA) and, in order to determine the major elements, 34 trace elements and rare earth elements, several analytical methods were used (for details see appendix G2 and www.actlabs.com). The quality of Actlabs's analyses was monitored by inserting two reference samples. Geochemical raw data (except for the gold) as reported by Actlabs were recalculated to a volatile free basis (for details of this transformation see Appendix 5 in Schlatter, 2007).
In total 46 drill core samples and 8 surface samples were collected and used for geochemical and petrographic investigations (Table 2). Fifty out of 54 rocks have been used for the lithogeochemical study, one rock was omitted because the sample is suspected to be contaminated with pegmatite material during sampling (sample 187532; appendix F) and three rocks (samples 187529, 187530 and 187540; appendix F) were omitted because they yielded unusual low titanium contents possibly due to analytical challenges.

Table 2. *Samples used for this study.*

Area	type of sample	Lithogeochemical samples	Petrographical samples	EMPA samples
Swan N	drill core for geochem analysis	16		
	drill core for petrography		7	
	drill core for microprobe			5
Swan	drill core for geochem analysis	10		
	rocks from surface for geochem analysis	8		
	rocks from surface for petrography		5	
	drill core for microprobe			1
Plateau	drill core for geochem analysis	20		
	drill core for petrography		11	
	drill core for microprobe			4
SUM		**54**	**23**	**10**

The mineralogy has been studied in 23 polished thin sections using a Zeiss "Axioskop 40" microscope in transmitted and reflected light. Ten sections were selected for microprobe analyses by a JEOL JXA-8200 superprobe at the Geological Institute in Copenhagen. Measurement was done at a beam current of 15 nA and an accelerating voltage of 15kV and counting time was 10 seconds on the peak and the background. Natural and synthetic oxides and silicates were used as standards and calibrations were performed on a routine basis. The analyses (242) were used to verify the minerals as identified by the optical microscope and to determine the chemistry of the main phases of the Qussuk rocks. The following major oxides were analysed with the superprobe: SiO_2, TiO_2, Al_2O_3, FeO as Fe total, MnO, MgO, CaO, Na_2O, K_2O and Cr_2O_3.

Work was also carried out with the Scanning Electron Microscope (SEM) at GEUS with a PHILIPS XL 40 SEM equipped with a ThermoNoran energy dispersive X-ray detection system. The purpose was to determine the chemical composition of spinel. For more details about the electron microprobe and SEM, the interested reader is referred to the homepages of the Geological Institute Electron microprobe laboratory and GEUS.

Geological and petrographical investigations of the Qussuk area

The Qussuk greenstone belt is about 20 km long, 2 km to 3 km wide and is divided from north to south into the Swan N, Swan and Plateau areas (Fig. 3). Detailed geological and petrographical descriptions of the host rocks of the gold mineralisation are provided for the Swan N and Plateau areas whereas in the Swan area lesser detailed work was carried out.

Swan N area

In the Swan N area, a 120 m thick rock sequence is studied from BH 24 (QUS08 DDH-24) and BH 25 (QUS08 DDH-25). BH 24 is 121.64 m long and BH 25 is 100.35 m long. Both bore holes were drilled from the same drill site at N 64.81080 W 51.09254 and with the same drill azimuth of 150° (Fig. 3a). BH 24 was drilled with an inclination of 45° and BH 25 with an inclination of 60°. Figure 5 provides the simplified geology of the drill profile from the Swan N area. The graphical logs are provided in appendix C. The bedding of the lithological units is moderately dipping at about 45° towards the north-west and the foliation is dipping between 52 and 59° north. The fabrics were measured from non oriented cores (appendix C). Because of the absence of way-up criteria in the rocks, it was not possible to identify the younging direction of the Swan N lithology and, consequently, the units above the Au-zone were defined as the structural hanging wall and the units below the Au-zone were defined as the structural footwall (Fig. 5). These main units are correlated between BH 24 and BH 25 and show that the Au-zone is parallel to the main foliation of the rocks.

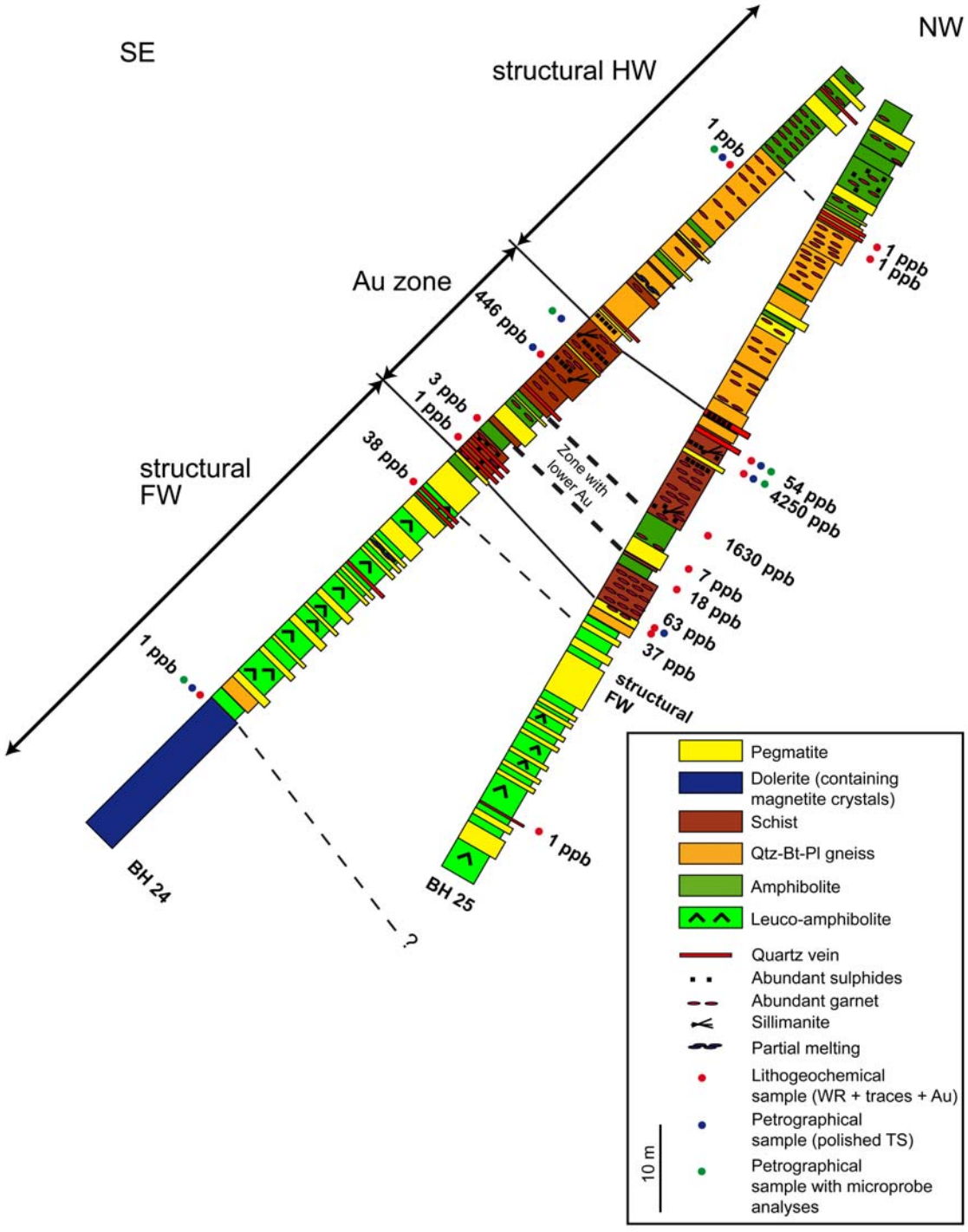

Figure 5. *Bore hole logs of BH 24 and 25 from Swan N. Only the gold contents from the lithogeochemical samples are shown. For the gold content of the continuous sampling done by NunaMinerals it is referred to appendix A.*

Structural Hanging wall

The structural hanging wall comprises about 15 m of dark grey, fine-grained amphibolite containing hornblende, plagioclase, quartz, garnet up to 1 cm in size, biotite and about 2 Vol. % sulphide specs. The lower part consists of about 25 m thick grey aluminous gneiss containing

quartz, garnet, biotite, plagioclase and locally spinel (Figs. 6a, 7a and b). Up to 10 cm wide zones with leucocratic pockets rich in quartz and feldspar likely represent melt veins (Fig. 5). The gneiss contains up to 5 Vol. % garnet which is up to 5 mm in size (Fig. 6a).

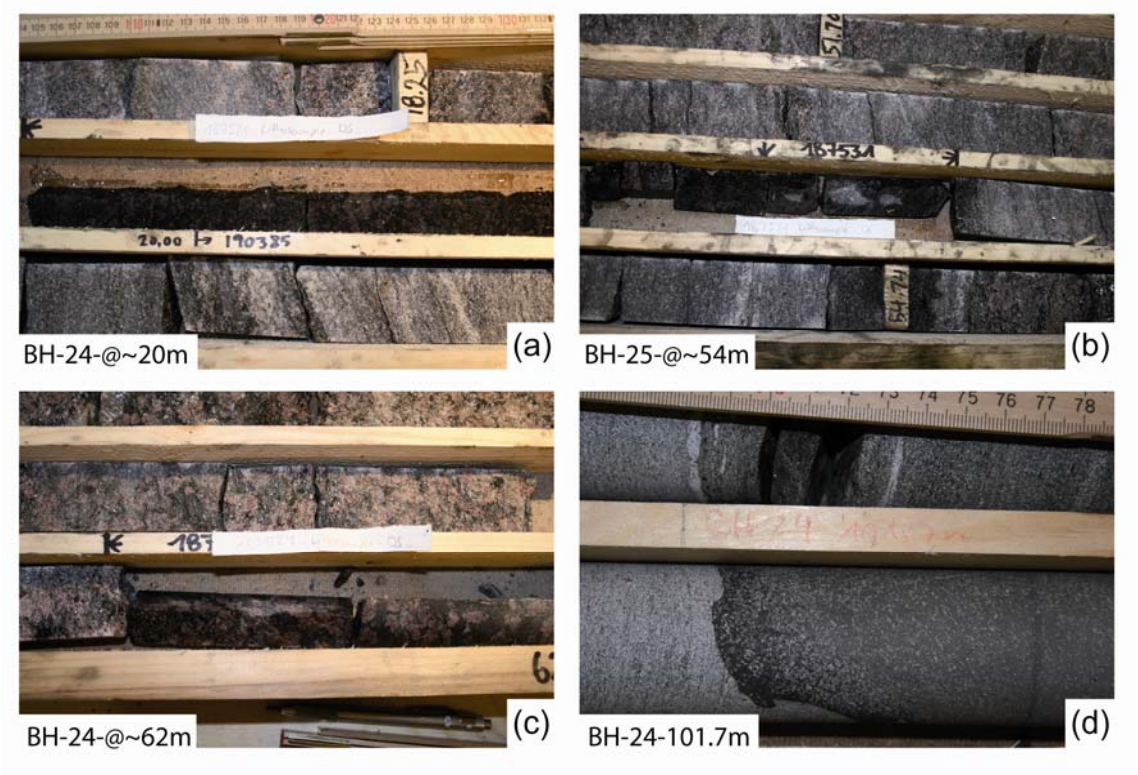

Figure 6. *Photographs from drill cores of BH 24 and 25 of the Swan N area. (a) BH-24-@~20m, Qtz-Bt-Pl-Grt gneiss of the structural hanging wall. (b) BH-25-@~54m, Bt-Grt schist of the Au-zone. (c) BH-24-@~62m, Grt-rich Bt schist of the Au-zone. (d) BH-24-101.7m, contact between leuco-amphibolite and dolerite dyke in the structural footwall.*

Garnet has minor compositional variations and is of the type Alm64Prp24Grs5Sps4. Plagioclase is andesine (For details of the microprobe analyzes see appendix D). The spinel has a Zn content of about 20 wt%, the FeO content is about 17 wt%, hence, the spinel has a composition between hercynite and gahnite (see appendix D for the details).
A few thin quartz veins and several 0.5 m to 2 m thick pegmatite dykes are also contained in the structural hanging wall.

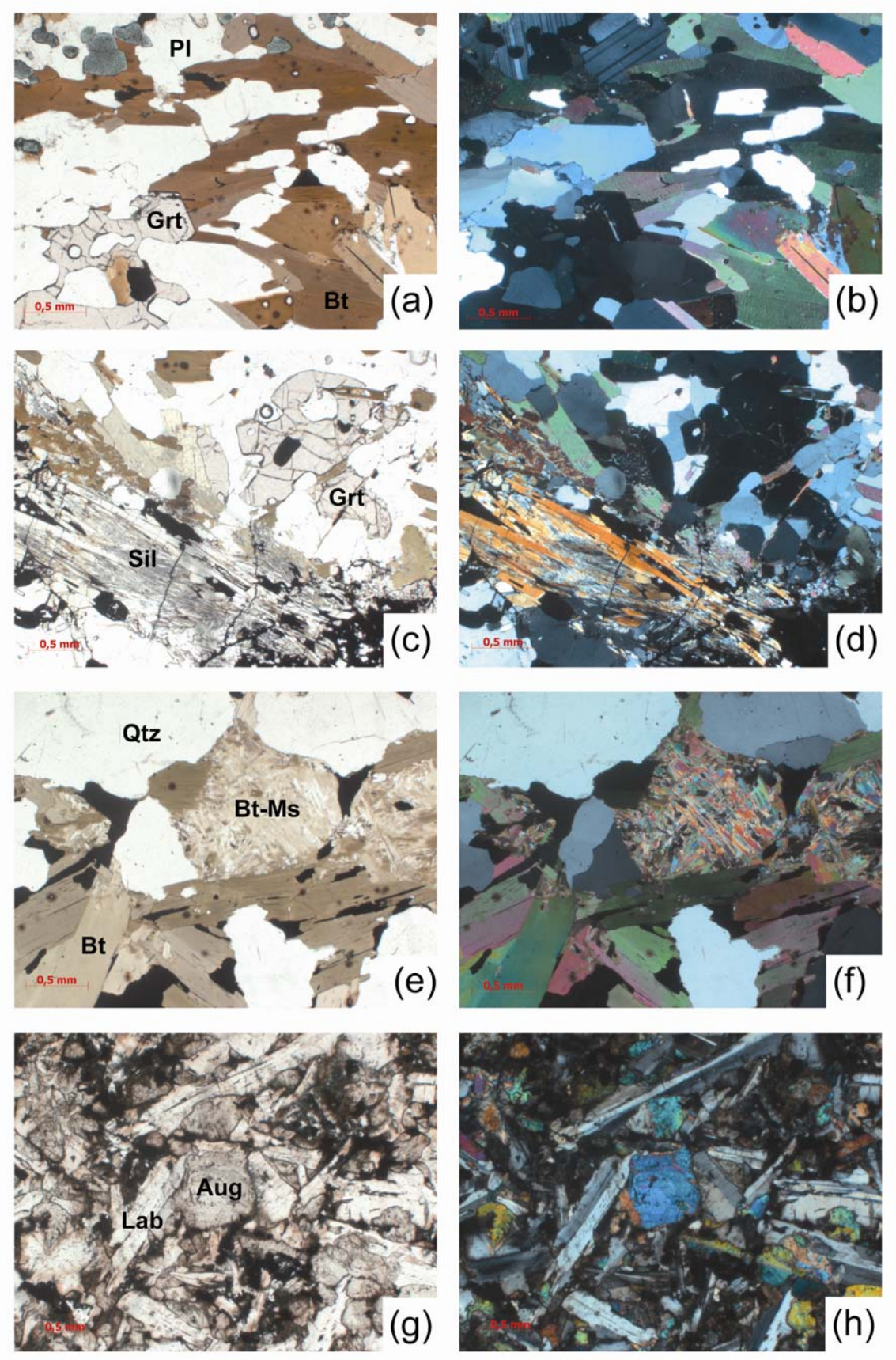

Figure 7. *Microphotographs from thin sections taken from drill cores of BH 24 and 25 of the Swan N area. (a and b) BH-25-45.35m, Swan N, structural hanging wall. Rock consists mainly*

of garnet, plagioclase and biotite. The green grains in (a) are spinel with a composition between hercynite and gahnite. (c and d) BH-25-43.3m Swan N, Au-Zone. Field of view shows mainly fibrous silimanite and garnet grains, biotite and quartz. (e and f) BH-25-45.35m, Swan N, Au-Zone. Intergrown biotite and muscovite replaces plagioclase (?); in a quartz-biotite-sulphide rich rock. (g and h) BH-24-102.35m Swan N, structural footwall. An ophitic texture of augite and labrodorite in the footwall-dolorite. (a, c, e and g = plane-polarized light; b, d, f, h = cross-polarized light).

Au-zone

Between the structural hanging wall and the structural footwall an interval of 21 to 25 m was defined as the Au-zone although within this zone some intervals have lower gold contents (Fig. 5). Careful sampling returned 1.24 ppm Au over 23 m and a shorter section within this zone contains 8.4 ppm Au over 2 m (Table 1).

The Au-zone consists mainly of biotite-quartz-garnet-sillimanite schist and hosts several foliation parallel quartz veins (Figs. 6b and c). These quartz veins are a few centimetres thick and contain up to 10 Vol. % sulphides. Another generation of quartz veins without sulphides and without gold is cross-cutting the foliation. Locally in the Au-zone quartz veining and rodding is seen and is interpreted as silicification. Sulphides occur in several bands of about 10 cm, in foliation-parallel stringers and are mainly pyrrhotite, chalcopyrite is less abundant. In the central part of the Au-zone, several thin amphibolite layers having lower gold content than the biotite schist (Fig. 5, Appendix A).

One quartz vein without sulphides occurs in BH 24, is 30 cm thick and crosscuts foliation and, similar to the structural hanging wall, crosscutting pegmatite dykes of up to 2 m occur in the Au-zone (Fig. 5). Petrographic observations show that the main minerals of the Au-zone are garnet, biotite, muscovite, sillimanite (of fibrolite type), plagioclase, pyroxene, amphibole, epidote and quartz (Fig 7c to f). Locally intergrown biotite-muscovite replaces plagioclase (Fig 7 e and f). This together with the silicification is interpreted as related to hydrothermal Au mineralisation. However, it is unclear if garnet and sillimanite are related to the same alteration stage.

Pyroxene is orthopyroxen with a composition between enstatite and ferrosilite; feldspar is oligoclase. The garnets have a composition between Alm55Prp14Grs3Sps21 and Alm72Prp18Grs2Sps5 (see appendix D).

Structural Footwall

The structural footwall consists of about 40 m massive grey, fine-grained leuco-amphibolite containing mainly hornblende, plagioclase, minor quartz and few 1 to 2 mm large garnet porphyroblasts (Fig. 5). This rock unit is intruded by numerous 1 to 5 m thick pegmatites. BH 24 intersects 20 m of a dark-green, homogenous, massive dolerite dyke rich in pyroxene and less abundant magnetite. At the immediate contact with the overlying leuco-amphibolite, a 5 mm thick chilled margin is seen (Fig. 6d). Petrographic observations reveal an ophitic texture for this dyke (Figs. 7g and h) with elongated, needle-shaped feldspar lattes that are labradorite and augite (Appendix D).

Plateau area

In the Plateau area, a 100 m thick rock sequence is studied from BH 02 (QUS08 DDH-02), BH 14 (QUS08 DDH-14) and from surface outcrops near the drill site. BH 02 is 121.64 m long and BH 14 is 100.35 m long. Both bore holes were drilled from the same drill site at N 64.66908 W 51.12211 and with the same drill azimuth of 270° (Fig. 3b). BH 02 was drilled with an inclination of 60° and BH 14 with an inclination of 45°. Figure 8 provides the simplified geology for the Plateau area and detailed graphic logs are provided in appendix C.

The bedding of the lithological units is steeply dipping at about 70 to 80° towards the east (Fig. 8) and foliation is dipping between 71 and 87° to the east. The fabrics were measured from non oriented cores (appendix C).

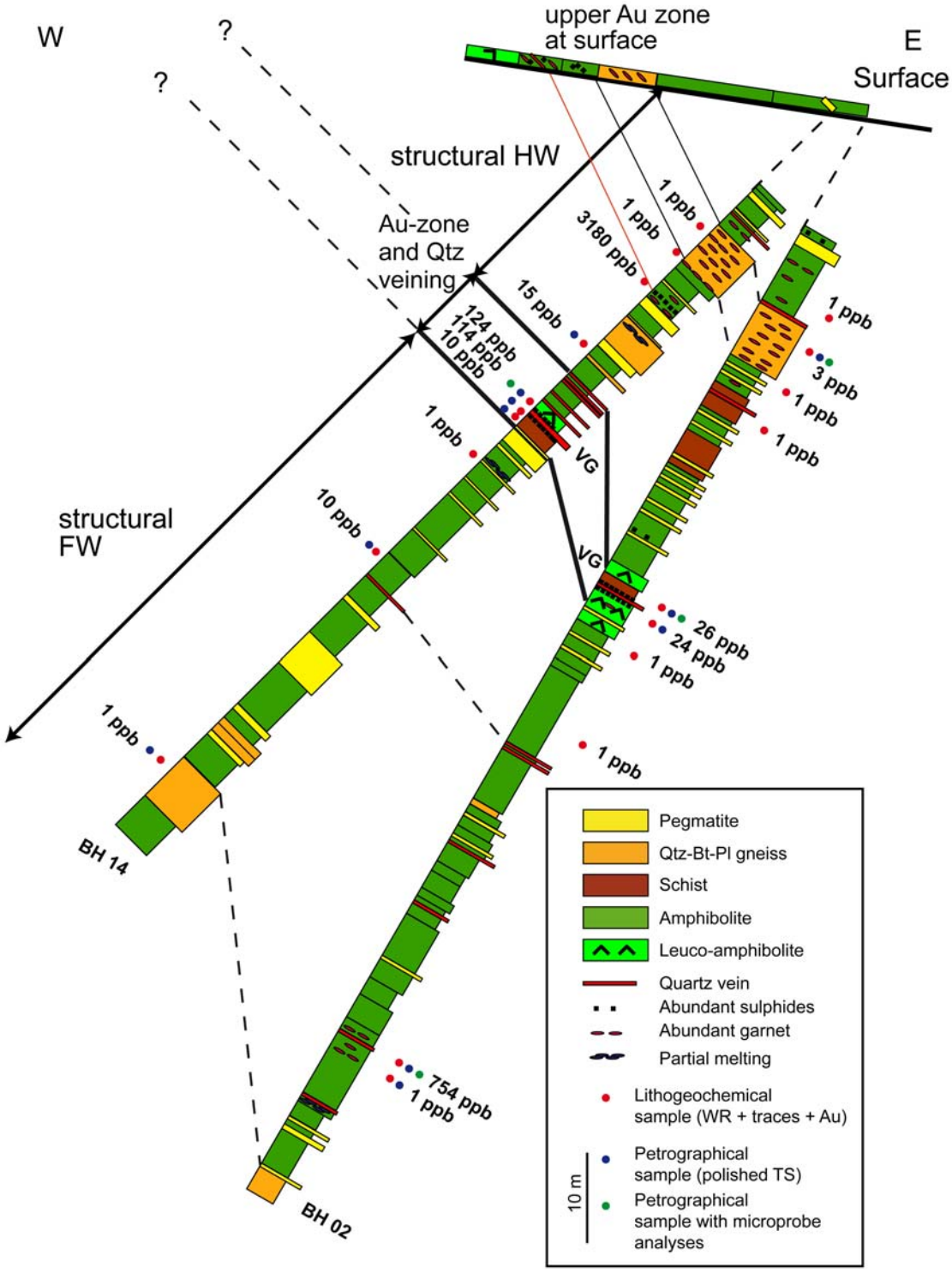

Figure 8. *Bore hole logs of BH 02 and 14 from Plateau. The geology is defined from the two bore holes and surface outcrops. Only the gold contents from the lithogeochemical samples are shown. For the gold content of the continuous sampling done by NunaMinerals it is referred to appendix A.*

Because of the lack of way-up criteria it was not possible to identify the younging direction of the lithology and, consequently, the units above the Au-zone were defined as the structural hanging wall and the units below the Au-zone were defined as the structural footwall (Fig. 8). The bedding of the lithological units is correlated between BH 02, BH 14 and the surface. The Au-zone is steeply dipping towards the east near parallel to the lithological units.

Structural Hanging wall

The structural hanging wall is about 40 m thick and consists mainly of fine- to medium-grained, greenish to dark greenish amphibolite.
This amphibolite contains mainly plagioclase, hornblende, garnet, quartz, calcite and apatite. Plagioclase is partially replaced by muscovite and hornblende and garnet is replaced by biotite. Muscovite and biotite together with pyrrhotite, chalcopyrite and gold (Fig. 8) are interpreted as hydrothermal alteration. One thin layer within the amphibolite comprises garnet and sulphides and contains up to 3.2 ppm gold over 0.2 m (Fig. 8; Appendix C).
Several 3 to 4 m thick units of biotite-quartz schist locally contain chalcopyrite and pyrrhotite. An unit about 7 m thick, in the upper part of the structural hanging wall, comprises dark-pinkish quartz-biotite-garnet-plagioclase gneiss. This aluminous gneiss does not contain any gold, is exposed on surface and is correlated with the drill profile (Figs. 8, 9 and 10a).

Figure 9. *Surface outcrop from Plateau at 735 m close to drill site of BH 02 and 14. This outcrop corresponds to the Qtz-Bt-Pl gneiss seen at surface (see orange coloured rock unit of figure 8)*

Garnet porphyroblasts of this aluminous gneiss are up to 1 cm in diameter and abundant (20 to 30 Vol. %). At surface and in the drill cores, the garnet-rich rocks have a reddish-pinkish colour (Figs. 9 and 10a).

Figure 10. *Photographs from drill cores of BH 02 and 14 of the Plateau area. (a) BH-02-13.8m, Qtz-Bt-Grt-Pl rich gneiss of the structural hanging wall. Garnet porphyroblasts have sizes of up to 1 cm (b) BH-14-37m, Quartz vein with visible gold of the Au-zone; one of the gold grains is encircled. (c) BH-02-@~46m, massive pyrrhotite of the inner alteration zone next to the quartz with VG of the Au-zone. (d) BH-14-@~59m, dark fine-grained biotite-hornblende-plagioclase-rich massive amphibolite of the structural footwall.*

Garnet has a composition between Alm52Prp24Grs0Sps1 and Alm68Prp26Grs3Sps1 and feldspar is mainly oligoclase (Appendix D). Anorthoclase occurs more rarely and biotite is locally replaced by retrograde chlorite (Figs. 11a and b).

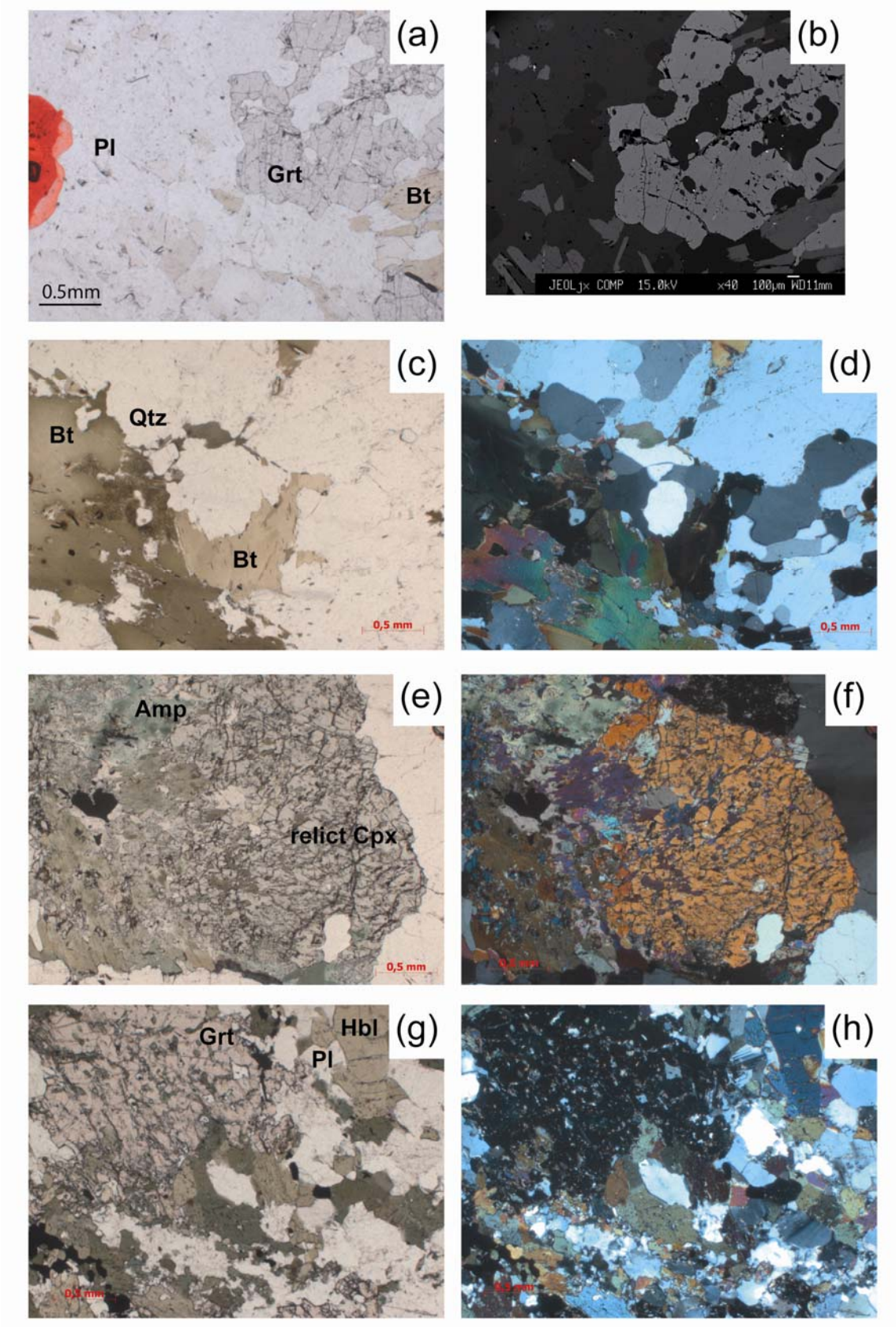

Figure 11. *Microphotographs from thin sections taken from drill cores of BH 02 and 14 of the Plateau area. (a and b) BH-02-13.95m, structural hanging wall. Rock consists mainly of garnet, plagioclase and biotite. In (b) the BSE image is shown, the large grain is garnet and the very small bright spots are monazite (c and d) BH-14-36.7m, Au-Zone. Rock comprises a thin quartz*

vein rimmed by biotite, Qtz and Bt are alteration minerals. (e and f) BH-02-45.95m, Au-Zone. A relict clinopyroxene is overgrown by amphibolite of actinolite type (Amp). (g and h) BH-02-101.6m, structural footwall. The amphibolite comprises garnet, plagioclase, hornblende quartz and sulphides (a, c, e and g = plane-polarized light; d, f, h = cross-polarized light, b = BSE image).

A medium-grained, beige-grey quartz-feldspar-rich gneiss of about 3 m thickness occurs in the deeper part of the structural hanging wall and pockets consisting of quartz and feldspar which are locally seen are interpreted as signs of in-situ partial melting.
A few quartz veins of about 10 cm and 0.5 m to 5 m thick pegmatite dykes occur in more or less regular intervals of a few metres (Fig. 8).

Au-zone

The Au-zone hosts several, about 10 cm wide, foliation parallel quartz veins, but only one of them shows visible gold (Fig. 10b). Sampling yielded 6.4 ppm Au over 1.1 m in BH 14 and 3.2 ppm Au over 2 m in BH 02 (Table 1). The quartz vein with VG is located at or close to the contact of leuco-amphibolite and amphibolite. Below and above the interval with the highest gold content, a several m wide halo with elevated gold occurs (Fig. 8). In detail, the quartz vein with VG is flanked by a few cm massive pyrrhotite (Fig. 10c). Below and above the pyrrhotite bands thin zones of brecciated, silicified, biotite-rich, and light green amphibolite occurs. These zones are interpreted as hydrobrecciation related to hydrothermal alteration (Appendix C). The proximal hydrothermal alteration zone therefore corresponds to the quartz vein with the pyrrhotite seams. The distal hydrothermal alteration zone corresponds to biotite-quartz schist. In the distal alteration zone, garnet, epidote and quartz occur together with biotite. In detail, a few centimetre thick quartz veins are rimmed by biotite (Fig. 11c) and epidote is intergrown with allanite (Fig. 12).

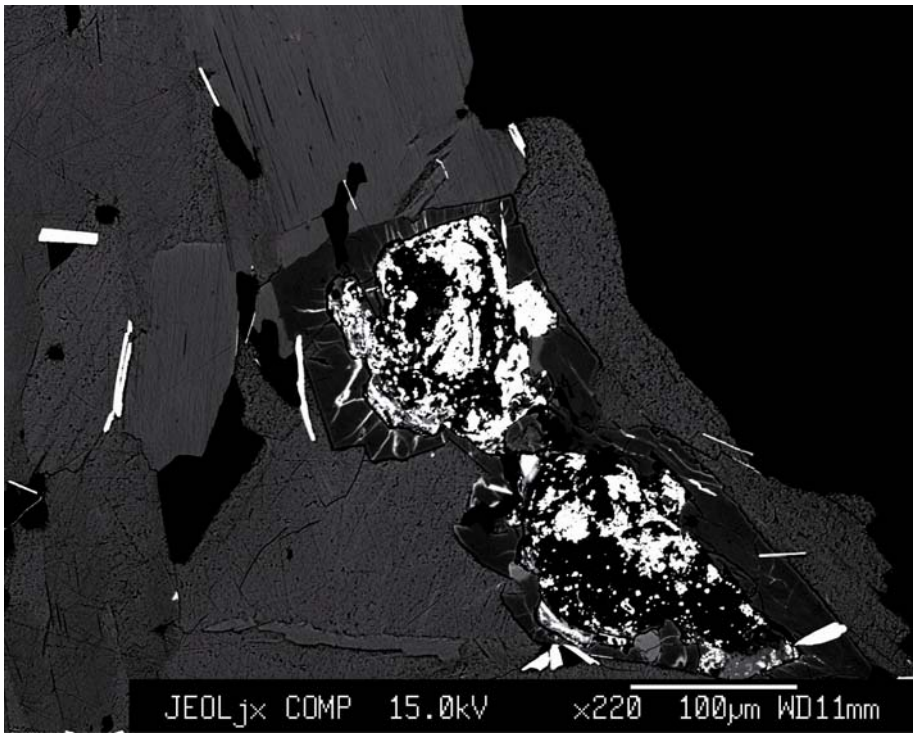

Figure 12. *BSE image of BH-14-36.7m from the Au-zone at Plateau. The patchy and needle shaped mineral with a very bright colour is allanite and the mineral around the allanite is epidote. Allanite from BH-14-36.7m could potentially be used for an age determination and would reveal the gold mineralisation age.*

Visible gold always occurs in a quartz vein flanked by pyrrhotite and chalcopyrite. NunaMinerals reported 7 drill intersections with quartz veins containing VG. These quartz veins are continuous along strike (at least on the target scale), were drilled down to about 60 m below surface in BH 18 and were interpreted to relate to shear zones (nunaminerals.com; Meddelelse nr 2008-35).

Structural Footwall

The structural footwall comprises about 70 m thick, dark amphibolite (Figs. 8 and 10d). Some layers are fine-grained, whereas other layers are medium-grained and some of the medium-grained layers contain garnet (Figs. 11 g and h). Partial melting is seen in amphibolite layers at the top and the bottom of the structural footwall (Fig. 8). One biotite-rich amphibolite layer of about 20 cm consists additionally of garnet, hornblende, plagioclase and quartz. A quartz vein is flanked by a garnet rich amphibolite and a 20 cm drill core sample of the amphibolite hosting the quartz vein yielded 754 ppb gold. The garnet has a composition between Alm52Prp9Grs22Sps5 and Alm62Prp12Grs16Sps5, the feldspar is bytownite and the amphibole is ferro-hornblende. Retrograde actinolite replaces garnet and plagioclase along their grain boundary (Appendix D).
Some layers of the deep structural footwall consist of quartz-biotite-feldspar gneiss.
Several up to 50 cm thick quartz veins with sharp contacts with the amphibolite host rock occur, but they never contain gold. By contrast to the quartz vein with VG of the Au-zone, distal and proximal alteration zones are not present and these veins should be excluded by the exploration model.
Several pegmatite dykes intruded the structural footwall; some of them are up to 4.5 m thick.

Swan area (area between Swan N and Plateau)

NunaMinerals drilled this target with four bore holes based on SkyTEM anomalies and because elevated gold contents were found on the surface in sediment and rock samples (Fig. 3a; Christensen 2010). However drilling returned only a few intersections above 100 ppb and none above 1 ppm Au. (Table 1; Appendix A).
In this study, BH 11(QUS08 DDH-11) was examined and 10 drill cores were sampled. These drill cores and 8 surface rocks were mainly collected for the lithogeochemical investigations (Fig. 13a).

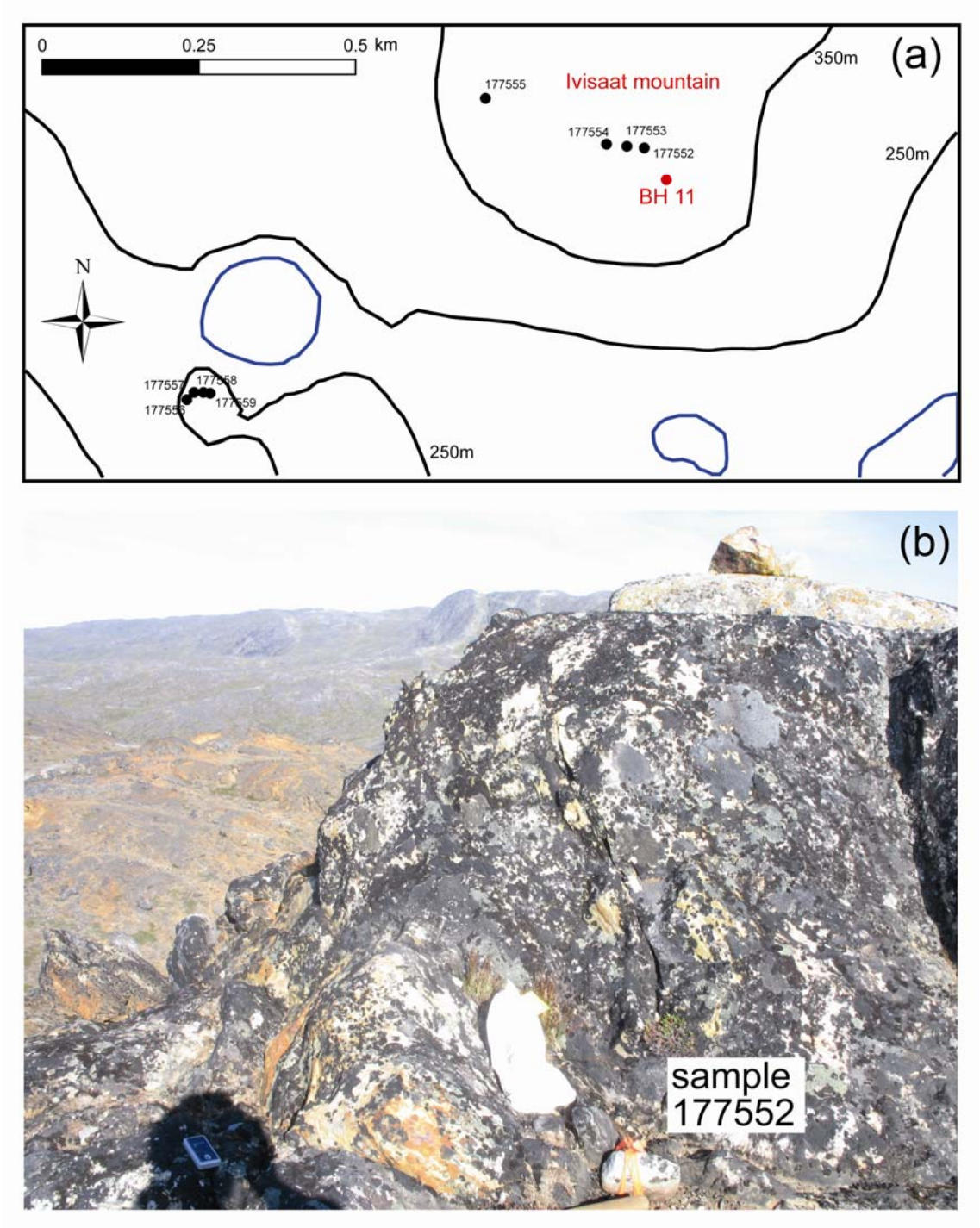

Figure 13. *Ivisaat mountain of the Swan Area. (a) Map shows location of bore hole BH 11 at 357 m above sea level. BH 11 is drilled with a dip of 80° to a depth of 300 m. Black circles indicate locations of the lithogeochemical samples taken from Ivisaat mountain and west of Ivisaat mountain. (b) Photo is taken at the location of sample 177552 at 397 m above sea level. The rocks seen at this location are massive and comprises quartz, sillimanite, fuchsite and garnet. The GPS seen in the lower left corner is about 8 cm large. More details of the outcrops are given in appendix B.*

In appendix B, the digital field data from the 8 surface samples from Swan are listed under stations *08DMS178* to *08DMS185*. The outcrops at and near the Ivisaat mountain (Fig. 13b) comprise massive rocks containing quartz, sillimanite, biotite, garnet, plagioclase, fuchsite (Cr-rich mica), and some layers are rich in tourmaline. Some of the rocks contain sulphides (Ccp, Py, Po) but the highest gold content is only 60 ppb (Appendices F and G-1). Although large areas in the vicinity of Ivisaat mountain are stained on surface (Fig 13b), these lithologies contain gold only below 1 ppm (Garde 2007, 2008; Fig. 3a). By contrast to the Swan N and the Plateau area, cordierite was reported from the Swan area from surface rocks (Garde 2008) and from bore holes (Fig. 14). It is interesting to note that in some areas of Qussuk cordierite is present, whereas in other areas it is absent and therefore represents a distinct difference of the sub areas. Cordierite does not appear to be associated with favourable alteration and with rocks elevated in gold.

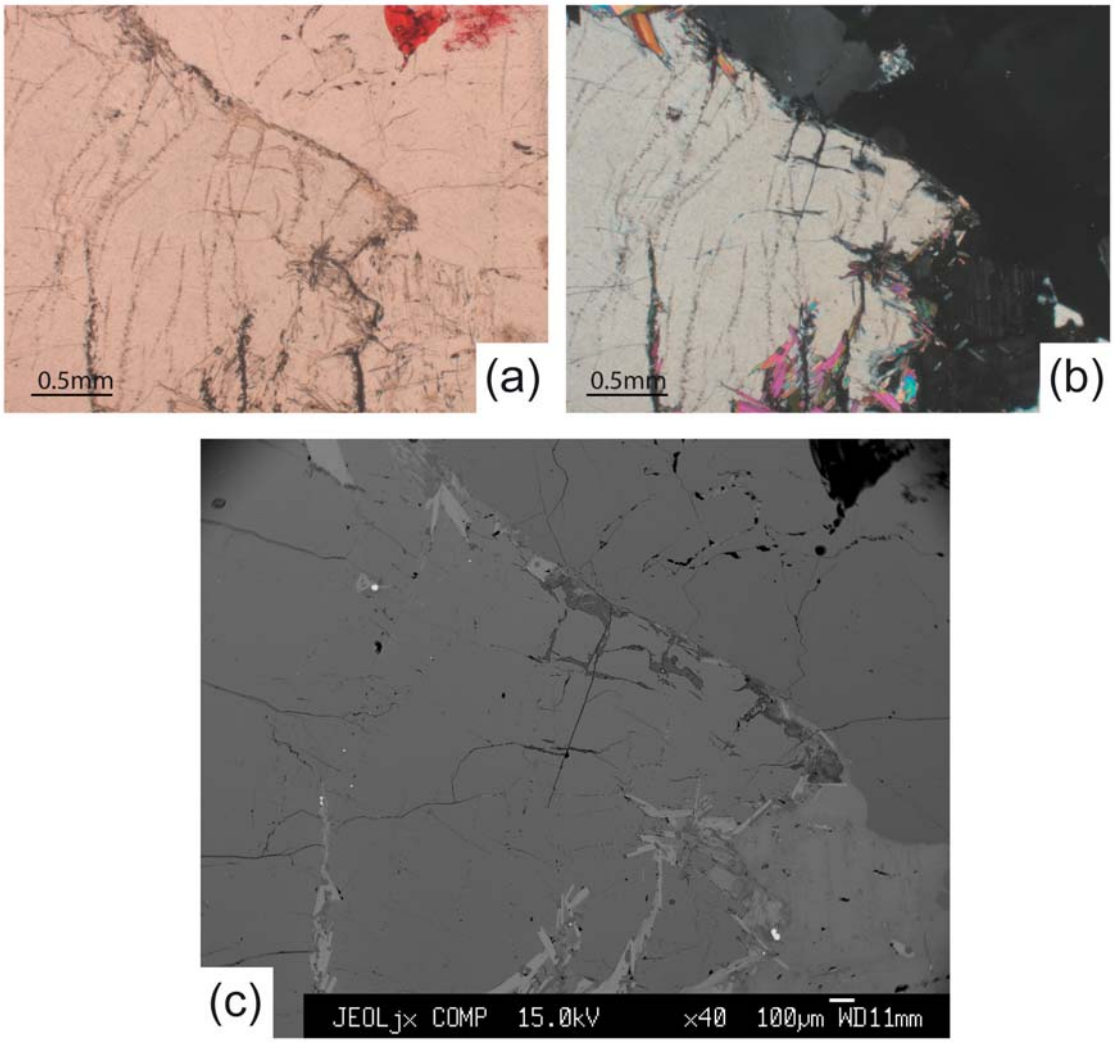

Figure 14. *(a and b): Microphotographs from a thin section taken from drill core of BH 11 of the Swan area at 16.9 m. The rock is quartz-biotite-cordierite schist containing pyrite and pyrrhotite and yields 61 ppb Au. The microphotograph shows a large cordierite grain (left half of the picture) and quartz (right half of the picture). Mica is seen on the edge of the cordierite grain and in some of the cracks within the cordierite (b). In (c) the BSE image of the same cordierite grain is shown. (a= plane-polarized light; b = cross-polarized light, c = BSE image).*

Correlation between drill cores, drill profiles and interpretation

The rock sequence of Plateau and Swan N are different and no straight forward geological correlation between the two areas can be made. However, the Au-zones in both areas are close to lithological contacts and contain quartz veins.

Biotite and muscovite replace plagioclase, biotite replaces garnet and small quartz veins are rimmed by biotite. The secondary minerals biotite, muscovite, quartz and sulphides are spatially associated with the gold-quartz veins and are therefore regarded as a product of hydrothermal alteration involving hydrothermal fluids rich in potassium, silica and iron.

Actinolite replacing pyroxene and chlorite replacing biotite likely represent retrograde metamorphism in greenschist facies. Because biotite is related to the hydrothermal alteration and the biotite is replaced by chlorite, retrograde metamorphism took place after the hydrothermal alteration.

By contrast, garnet-rich gneiss in the structural footwall only contains gold in the ppb range. The lack of quartz veins, gold and hydrothermal alteration suggests that the garnet is not related to the hydrothermal stage which has introduced the gold at Qussuk.

In the Swan area, quartz veins are absent, metamorphic minerals such as e.g. cordierite and sillimanite are more dominant than biotite and until now no economically interesting gold mineralisation has been found at Swan.

Chemical rock definition

Because most rocks of the Qussuk area are metamorphosed and hydrothermally altered, diagrams based on mobile major oxides, such as, e.g., the total alkali-silica diagram or diagrams based on SiO_2 and Zr/TiO_2 cannot be applied to classify the rocks (Le Bas et al. 1986). A way to get around this dilemma is to apply rock classification diagrams using immobile element ratios because effects of hydrothermal alteration are obliterated (MacLean and Barrett, 1993). Fig 15a shows a discrimination diagram based on immobile element ratios and reveals that the rocks from Qussuk fall mainly into the basalt and andesite fields. Rocks from the different sub areas (Swan N, Swan and Plateau) are chemically very similar (Fig. 15b, c, d).

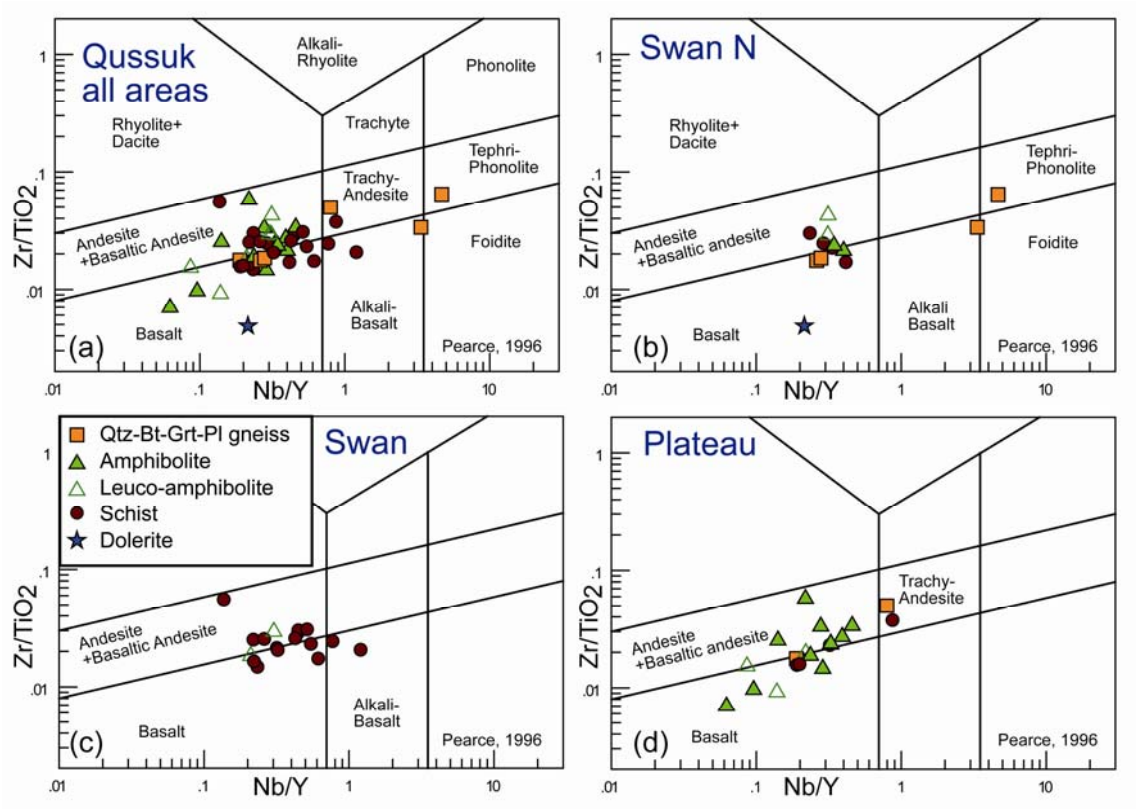

Figure 15. *(a,b,c and d): Rocks are classified in a plot based on the immobile element ratios Nb/Y and Zr/TiO_2 (Winchester and Floyd, 1977; revised by Pearce, 1996). The discrimination plots makes it possible to classify rocks which were described in the field as dolerite, schist, leuco-amphibolite, amphibolite and gneiss into basalt, basaltic andesite and andesite, trachy-andesite, alkali basalt and tephri-phonolite. In (a) samples from all areas are shown and it can be seen that all samples from Qussuk are basic or intermediate. Rocks from Swan N (b), Swan (c) and Plateau (d) are similar. Legend is given in (c).*

Refined chemical rock definition

In order to further classify the rocks with the aim to establish the chemostratigraphy, the rocks were chemically classified based on Al_2O_3/TiO_2, Zr/Al_2O_3 and Zr/TiO_2 ratios. In the Qussuk areas, 10 chemical groups were identified: andesite A, andesite B, basaltic andesite I, basaltic andesite II, basalt X, basalt A, basalt B, basalt C, basalt D and dolerite. Plots of one immobile-element ratio versus another removes mass change effects caused by hydrothermal alteration and the chemical groups form fairly tight clusters (Fig. 16).

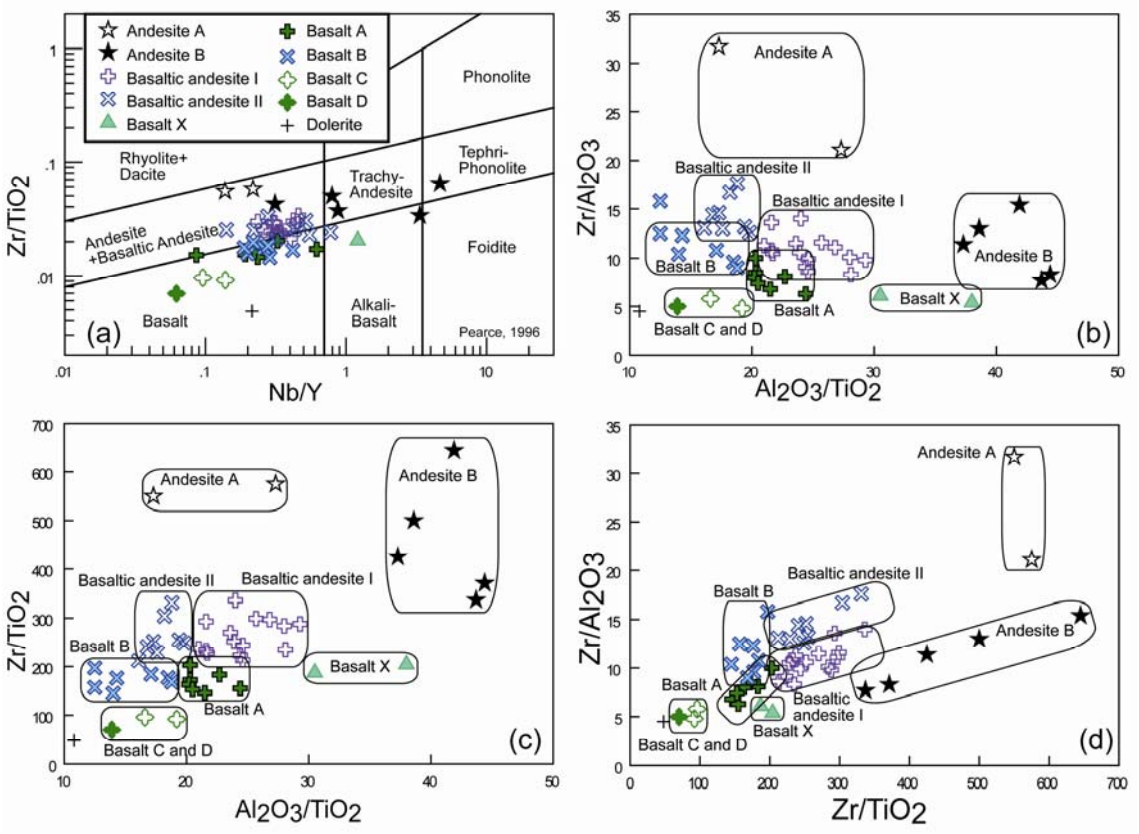

Figure 16. *Immobile element ratio-ratio plots. (a) The samples from Qussuk fall into the basalt and basaltic andesite/andesite fields (Winchester and Floyd, 1977; revised by Pearce, 1996). (b) The chemical groups form fairly tight clusters in a diagram based on Al_2O_3/TiO_2 versus Zr/Al_2O_3 diagram. (c) The chemical groups form fairly tight clusters in a diagram based on Al_2O_3/TiO_2 versus Zr/TiO_2 diagram. (d) The chemical groups form fairly tight clusters in a diagram based on Zr/TiO_2 versus Zr/Al_2O_3 diagram.*

Table 3 lists the criteria which were used to classify each rock into one of these chemical groups and appendix H provides the chemical rock type for all the samples of this study. [These criteria as shown in Table 3 can be used in the future to classify new lithogeochemical samples from Qussuk].

Table 3. *Chemical rock types and characteristic immobile-element ratios used for definition. REE data were corrected to a volatile free basis, then normalized to the chondrite values of Evensen et al. (1978)*

Chemical groups:	Mean and St. deviation	Al_2O_3 /TiO_2	Zr/ Al_2O_3	Zr/TiO_2	Zr/Y	Zr/Nb	Nb/Y	Zr/10*P_2O_5	Lan/Ybn
Andesite A	**mean**	22,3	26,4	563	7,8	46,1	0,18	3,6	6,7
n=2	**st. dev**	5,0	5,3	12	0,2	11,7	0,04	1,0	0,6
Andesite B	**mean**	41,2	11,2	455	56,6	34,5	1,99	1,7	50,2
n=5	**st. dev**	2,6	2,5	94	33,5	10,4	1,59	0,9	26,7
Basaltic Andesite I	**mean**	24,6	10,7	262	10,4	29,4	0,35	2,7	15,9
n=15	**st. dev**	2,0	1,2	31	3,0	4,5	0,05	1,0	13,0
Basaltic Andesite II	**mean**	18,0	14,4	259	11,3	29,0	0,40	2,3	11,6
n=8	**st. dev**	1,0	1,4	29	3,9	5,3	0,16	1,1	3,9
Basalt X	**mean**	34,3	5,7	196	20,7	28,8	0,73	1,3	17,8
n=2	**st. dev**	3,7	0,4	9	13,8	0,3	0,49	0,2	1,2
Basalt A	**mean**	21,4	7,9	168	7,8	30,6	0,27	1,4	5,9
n=7	**st. dev**	1,3	0,9	16	3,7	6,9	0,11	0,3	2,4
Basalt B	**mean**	15,4	11,5	172	6,3	24,6	0,27	3,8	10,1
n=7	**st. dev**	2,3	1,8	13	0,8	2,8	0,05	1,6	5,4
Basalt C	**mean**	17,9	5,3	94	3,0	26,6	0,12	0,9	1,5
n=2	**st. dev**	1,3	0,5	2	0,1	5,7	0,02	0,0	0,1
Basalt D (n=1)		13,9	5,0	70	2,4	38,3	0,06	0,7	1,3
Dolerite (n=1)		10,8	4,5	48	2,5	11,5	0,22	0,9	3,9

In order to assess if the areas Swan N, Swan and Plateau comprise different rock types, samples from each area were plotted in immobile element ratio plots (Fig. 17). It is shown that most of the rock types occur in all of the areas; but there are also distinct differences: e.g. basalts C and D occur only in the Plateau area (Fig. 17c); basalt X only occurs in the Plateau and Swan area (Figs. 17b and c) and andesite A only occurs in the Swan and Plateau areas (Fig. 17b and c).

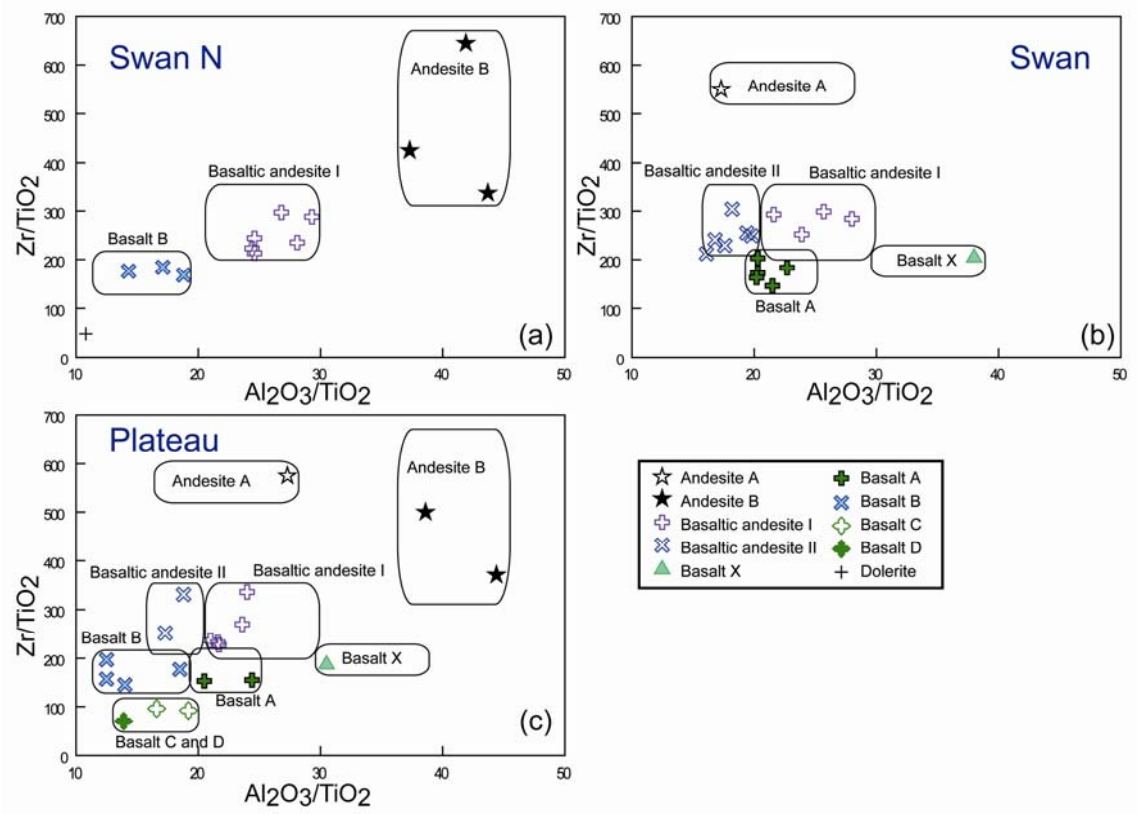

Figure 17. *Immobile element ratio-ratio plots for rocks from Swan N, Swan and Plateau areas. (a) The Al_2O_3/TiO_2 versus Zr/TiO_2 diagram shows that in Swan N the rock types andesite B, basaltic andesite I, basalt B and dolerite occurs. In Swan (b) andesite A, basaltic andesite I, basaltic andesite II, basalt A and basalt X occurs and in Plateau (c) all the 10 rock types except dolerite occurs.*

Magmatic Affinity

The magmatic affinity was defined by the Zr/Y ratios (MacLean and Barrett 1993, Barrett and MacLean 1994). Figure 18a shows that most of the rocks are calc-alkaline or transitional and only few rocks are tholeiitic. Least altered tholeiitic rocks have flat REE patterns, and calc-alkaline rocks show steeper REE patterns (Figs. 18b, c and d). A diagram based on the La_n/Yb_n and Zr/Y ratio shows that the rocks are mainly of calc-alkaline and transitional magmatic affinity and that some rocks are strongly calc-alkaline (Fig. 19a).

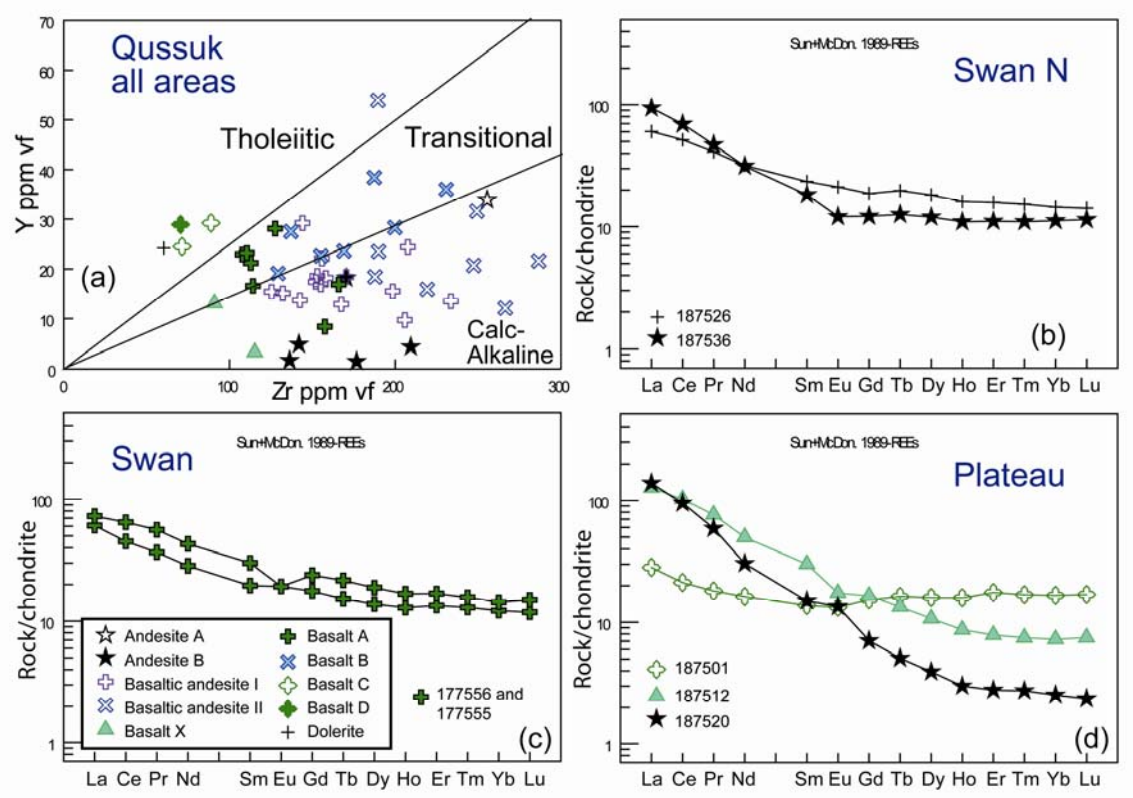

Figure 18. *Magmatic affinity for all Qussuk samples. (a) A diagram based on Zr and Y shows that most of the Qussuk samples are calc-alkaline and transitional; only a few samples plot in the tholeiitic field. (b) Least altered samples from Swan N: a chondrite-normalized plot shows that the pattern for andesite B is relatively steep from La to Eu, then relatively flat to Lu which is typical for rocks of calc-alkaline magmatic affinity. The dolorite sample shows a tholeitic affinity. (c) Least altered samples from Swan: two basalt A samples show transitional magmatic affinity. (d) Least altered samples from Plateau: the flat pattern of the basalt C is typical for a tholeiitic magmatic affinity and basalt X and andesite B show calc-alkaline and mildly calc-alkaline affinity. Legend of a, b and d is shown in c. REE data were corrected to a volatile free basis, then normalized to the chondrite values of Sun and McDonald (1989). (vf = volatile free basis; details of the samples used can be found in appendix F).*

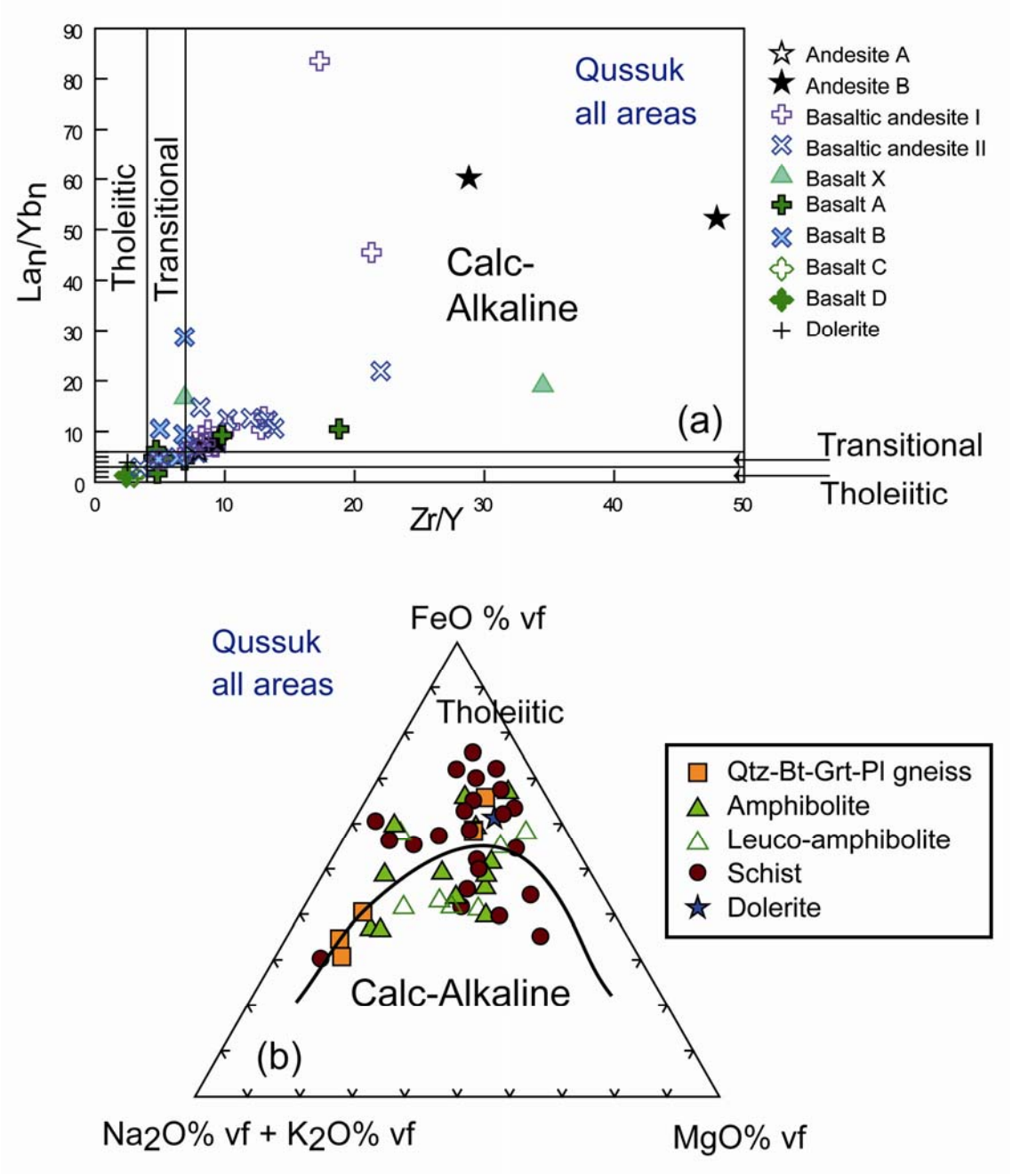

Figure 19. *(a) The magmatic affinity is assessed by using a plot based on Zr, Y, La and Yb. Samples are of calc-alkaline, transitional and tholeiitic magmatic affinity; several rocks are strongly calc-alkaline with Zr/Y ratios >30. REE data were corrected to a volatile free basis, then normalized to the chondrite values of Evensen et al. (1978) (b) Samples from all Qussuk areas are plotted into a AFM diagram. (vf = volatile free basis, for details see text).*

In the Swan N area, the rocks are mainly calc-alkaline and a few are tholeiitic or transitional. In the Swan area, the rocks yield a transitional or calc-alkaline affinity and in the Plateau area the rocks are calc-alkaline or transitional and a few are tholeiitc (Appendix F).

The same rocks were also plotted in an AFM diagram (Fig. 19b) and yield calc-alkaline or tholeiitic affinity. About half of the biotite-schist plot in the tholeiitic field, although they have calc-alkaline affinity (Fig. 18a) and substantiate that classification diagrams based on mobile major oxides are not appropriate for hydrothermally altered rocks.

Chemostratigraphy

Figure 20 shows the lithological units of the Swan N and the Plateau areas and the chemical rock types of all the samples. This diagram allows defining the chemostratigraphy:

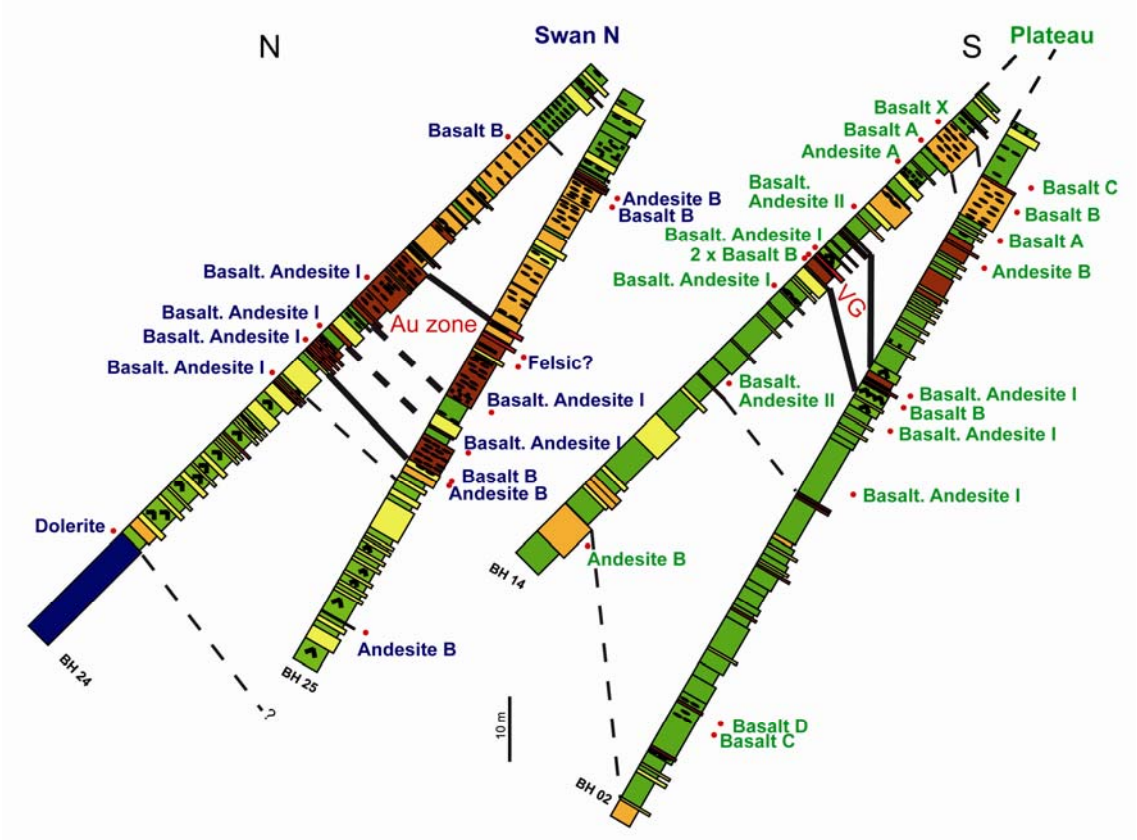

Figure 20. *Chemostratigraphic relation on Swan N and Plateau sections. Distance between Swan N in the north and Plateau in the south is about 16 km. Some correlations is possible; e.g. basaltic andesite I occurring in the Au-zone can be correlated between the drill holes of each section. For legend see figure 5.*

At *Swan N* the structural hanging wall comprises basalt B and andesite B. The Au-zone comprises mainly basaltic andesite I, and the structural footwall andesite B. In the *Plateau area*, the structural hanging wall contains different varieties of basalts, andesites and basaltic andesite II. The Au-zone in the Plateau area comprises basaltic andesite I and basalt B, and the structural footwall contains basaltic andesite I and II, andesite B and basalt D and C.
The most abundant rock type of the Au-zone in the Plateau area as well as in the Swan N area is basaltic andesite I. This chemostratigraphic interval is a good marker unit and could represent an ore horizon, or a favourable unit on the regional scale. Figure 21 shows that basaltic andesite I rocks define a distinct field in a ternary diagram based on three immobile element ratios.

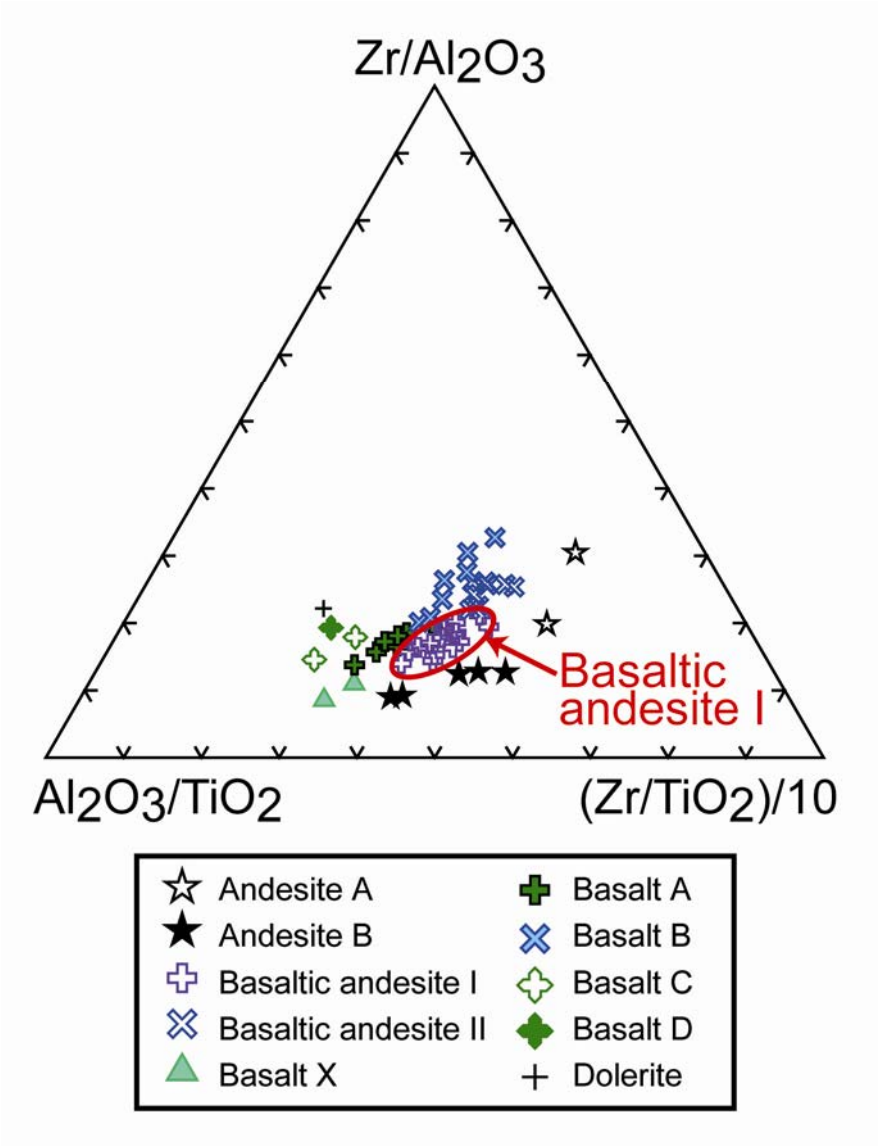

Figure 21. *A ternary plot based on the ratios Zr/Al_2O_3, Al_2O_3/TiO_2 and $(Zr/TiO_2)/10$ reveals that the 10 chemical groups form fairly tight clusters. The basaltic andesite I samples which occurs in the Au-zones of Swan N and Plateau are contoured and the field of basaltic andesite I is located in the lower middle part of the ternary plot.*

Identifying basaltic andesite I rocks in other profiles can help to identify additional favourable units in other areas. The mineralogy of the basaltic andesite I rocks is characterised by the primary minerals plagioclase, quartz hornblende and garnet and the alteration minerals are biotite, quartz and sulphide. In some of the basaltic andesite I rocks sillimanite, titanite, actinolite and diopside also occur, but further work is necessary to assess if these are primary metamorphic or hydrothermal alteration minerals.

Correlation between Au and Ag, Cu, Zn; and metal ratios

A ternary plot based on gold and the base metals Cu, Zn, Pb and Ag can be used to discriminate between auriferous and base metal massive sulphide deposits (Poulsen and Hannington 1995). It has earlier been suggested that the Qussuk gold mineralisation is an auriferous massive sulphide deposit (Andreasen 2007). The data used for this report however, indicate that the Qussuk gold mineralisation is not an auriferous massive sulphide deposit because the samples fall outside the field of auriferous massive sulphide deposit (Fig. 22a and appendix A).

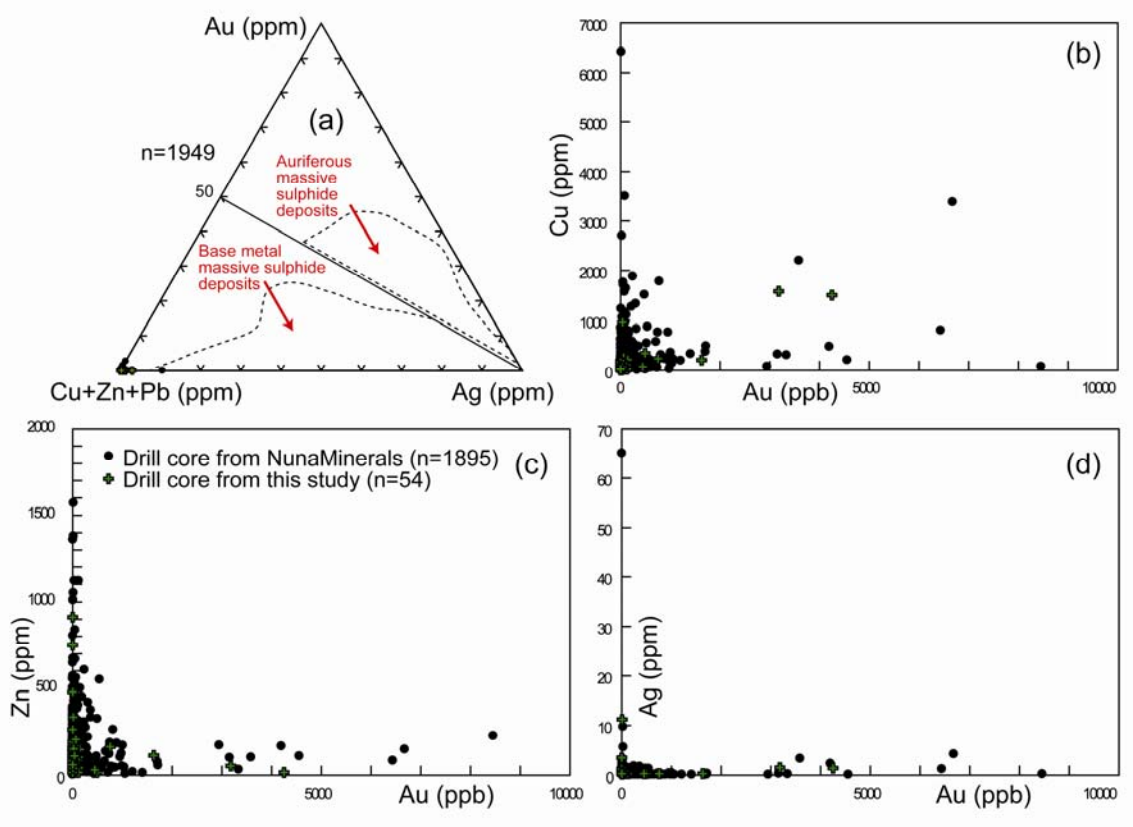

Figure 22. *(a) Ternary plot based on Au, Cu, Zn, Pb and Ag. Qussuk samples are not characteristics for massive sulphide deposits as they are plotting outside these fields (Poulsen and Hannington, 1995). (b, c, d) Au is not correlating with Cu, Zn or Ag. (d) Ag contents of the Qussuk samples are very low.*

Au and Cu as well as Au and Zn show no correlation (Fig. 22b and c). Figure 22 d shows that Ag contents are low and that no correlation between Au and Ag exists.

Base metal contents are generally low; and arsenic contents are very low (generally below 5 ppm). The low As content of the Qussuk gold mineralisation is a distinct difference of the nearby Storø gold mineralisation which generally has elevated As content (Knudsen et al. 2007).

Alteration; as seen from TiO_2 versus Zr plots

It has been shown in an earlier section that the hydrothermal alteration minerals of the Au-zone are mainly quartz, biotite, muscovite and sulphide.
On a TiO_2 versus Zr diagram, rocks belonging to the same chemical group form alteration lines (MacLean and Barrett 1993). Hydrothermal alteration has caused mass gains or losses of the mobile elements in the rocks which in turn results in dilution or residual concentration of the immobile elements. However, these effects do not change the initial ratio between two immobile elements for a given chemical rock type. Some rock types such as e.g. basalt A, and andesite B are only moderately altered because they rather form clusters than that they form alteration lines (Fig. 23a).

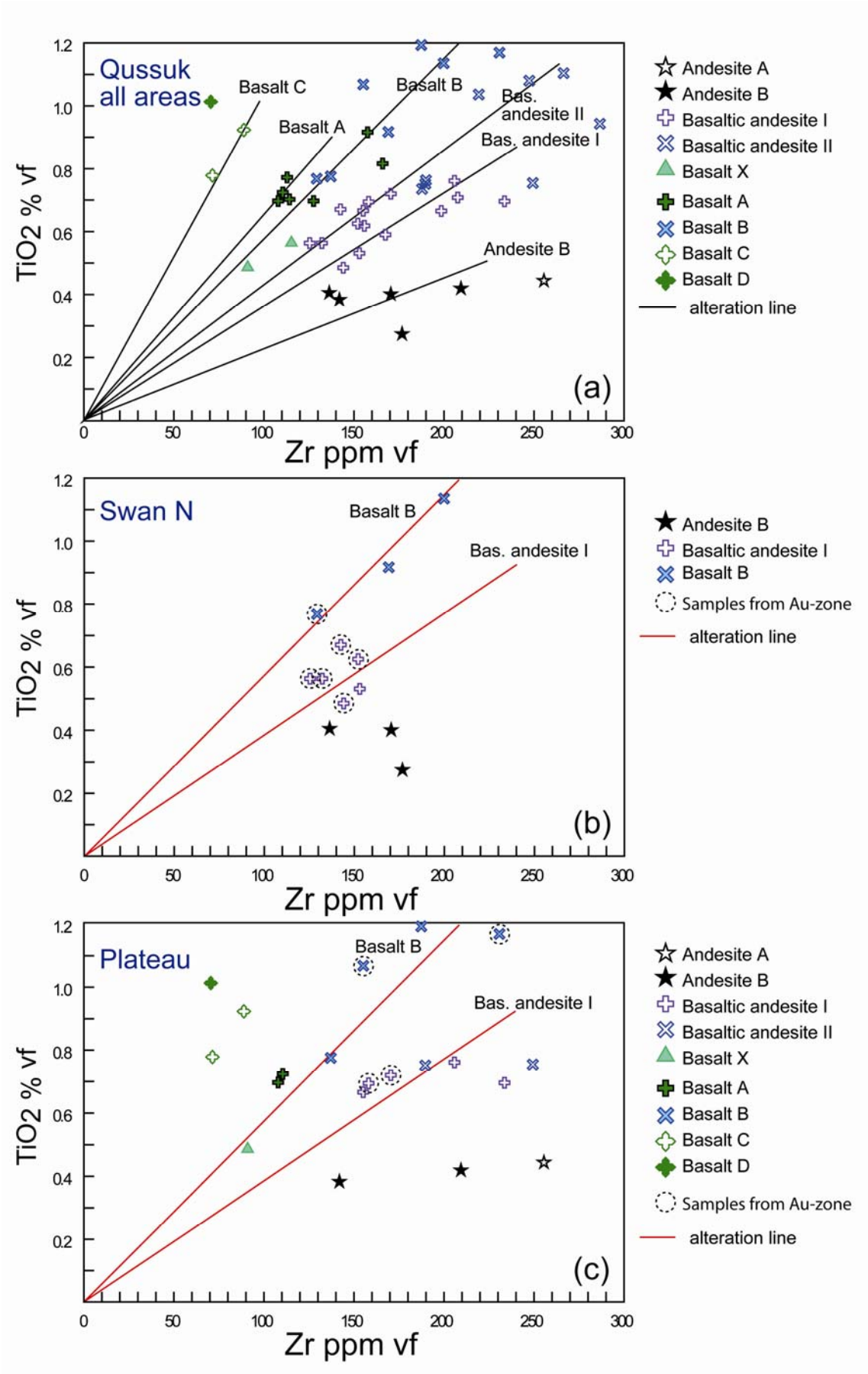
Qussuk
all areas
Basalt C
Basalt A
Basalt B
Bas.
andesite II
Bas. andesite I
Andesite B
(a)
TiO2 % vf
Zr ppm vf
Andesite A
Andesite B
Basaltic andesite I
Basaltic andesite II
Basalt X
Basalt A
Basalt B
Basalt C
Basalt D
alteration line
Swan N
Basalt B
Bas. andesite I
(b)
Samples from Au-zone
Plateau
(c)

Figure 23. *A Zr vs TiO_2 plot is used to estimate the intensity of the hydrothermal alteration. Altered samples define elongated fields. (a) All Qussuk samples except of the unaltered dolerite sample are plotted in a Zr vs. TiO_2. (b) Swan N samples from the Au-zone are similarly altered than samples located outside the Au-zone. (c) Plateau samples from the Au-zone are similarly altered than samples located outside the Au-zone. (vf = volatile free basis).*

On the other hand, basaltic andesite I and basalt B, form distinct alteration lines and are, therefore, more altered then the other rock types. Basaltic andesite I and basalt B are both rock types which occur in the Au-zone of the Swan N and Plateau area. Basaltic andesite I and basalt B of the Swan N and Plateau show very similar alteration trends (Figs 23b and c), hence they likely were subjected to similar alteration intensities.

Discussion and conclusions

The rock sequence of Plateau and Swan N are different and no straight forward geological correlation between the two areas can be made. However, the Au-zones occur in both areas close to lithological contacts. In the Swan N area, the Au-zone is located between Qtz-Bt-Pl gneiss in the hanging-wall and leuco-amphibolite in the footwall whereas in the Plateau area, the Au-zone is located between leuco-amphibolite in the hanging-wall and amphibolite in the footwall (Fig. 20). Application of immobile-element methods to 50 whole-rock analyses show that the rocks from Plateau, Swan and Swan N can be classified into 10 different chemical groups ranging from andesite to basalt with transitional to calc-alkaline affinity, and only few are of tholeiitic magmatic affinity. The rock show characteristics of rocks formed in an island arc complex (Garde 2007). Interestingly, the volcanic rocks from the Qussuk area are mafic to intermediate, whereas felsic rocks are not part of the lithology. The lack of felsic rocks does not support earlier work, which suggested that the Qussuk gold mineralisation represents a volcanic-hosted massive sulphide (VMS) deposit (Andresen 2007). The close spatial association with a felsic volcanic centre is characteristic for this deposit class (Schlatter 2007) and VMS deposits entirely hosted in mafic to intermediate rocks are generally related to ophiolite complexes (Galley and Koski 2000). Rocks from the nearby Storø island (Fig. 2) are geochemically similar to the Qussuk rocks and comprise mainly basalts (Knudsen 2007).

Au-zones of Plateau and Swan N both comprise biotite-muscovite-quartz-sulphide alteration zones containing quartz veins, although in Plateau, this zone is narrower than in the Swan N area. In detail, the inner alteration zone is characterised by quartz, VG (only at Plateau) and massive to disseminated pyrrhotite (± biotite). In the intermediate alteration zone biotite and quartz occur. Garnet and sillimanite seen in the intermediate alteration zone at Swan N might or might not be caused by hydrothermal alteration. The outer alteration zone is defined by biotite and disseminated sulphide and extends for a few metres and the transition to unaltered metamorphic rocks is gradual.

Although the alteration zonation of the Swan N and Plateau area is similar, the extend of the alteration zones differs. It is conceivable that the alteration zones are narrower in the Plateau area and wider in the Swan N because the areas represent wider and narrower shear zones and in turn focus alteration fluids differently. Enveloping and symmetric alteration zones around gold mineralisation is typical for orogenic gold deposits (Eilu and Groves 2001) and represents a distinctive feature from other deposit types such as VMS deposits (Schlatter 2007).

Minerals such as sillimanite and garnet are interpreted to be the result of metamorphism of hydrothermally altered rocks (Garde 2008). However, these minerals may as well have formed from an Al-rich sediment precursor during metamorphism and without involvement of hydrothermal alteration. Also the garnet-rich zone was explained to be the altered equivalent from amphibolites which are above and below the garnet-rich rocks. This is not supported by the lithogeochemical data because detailed lithogeochemistry has shown that the garnet-rich rocks have a variable composition containing basalt B, basalt X and basalt A, and the amphibolite above and below are basalt C, basalt X and andesite A (Fig. 20) which means that the amphibolite cannot be the precursor of the garnet-rich rock.

The presence of plagioclase suggests that these rocks are not strongly altered or extremely leached, because strong alteration would cause breakdown of plagioclase due to leaching of the mobile elements Na and Ca.

Although the rocks from the gold zone of the Swan N area and the Plateau area are similar, in detail they have variable composition. Whole rock analyses from the Au-zone, reveal that Na_2O contents of rocks from the Swan N area yield in average 0.6 wt% and from the Plateau area the

average content is 3.3 wt%. CaO average contents are 2.8 wt% for Swan N and 5.6 wt% for Plateau respectively. K_2O contents of the samples from the Au-zone are generally elevated (in average 2.14 wt% for Swan N and 1.87 wt% for Plateau) and support that biotite is a result of post-peak metamorphic hydrothermal alteration. Potassium metasomatism is a characteristic feature of orogenic gold deposits (Groves et al. 2003). The Au-zone also has elevated silica contents (Fig. 24).

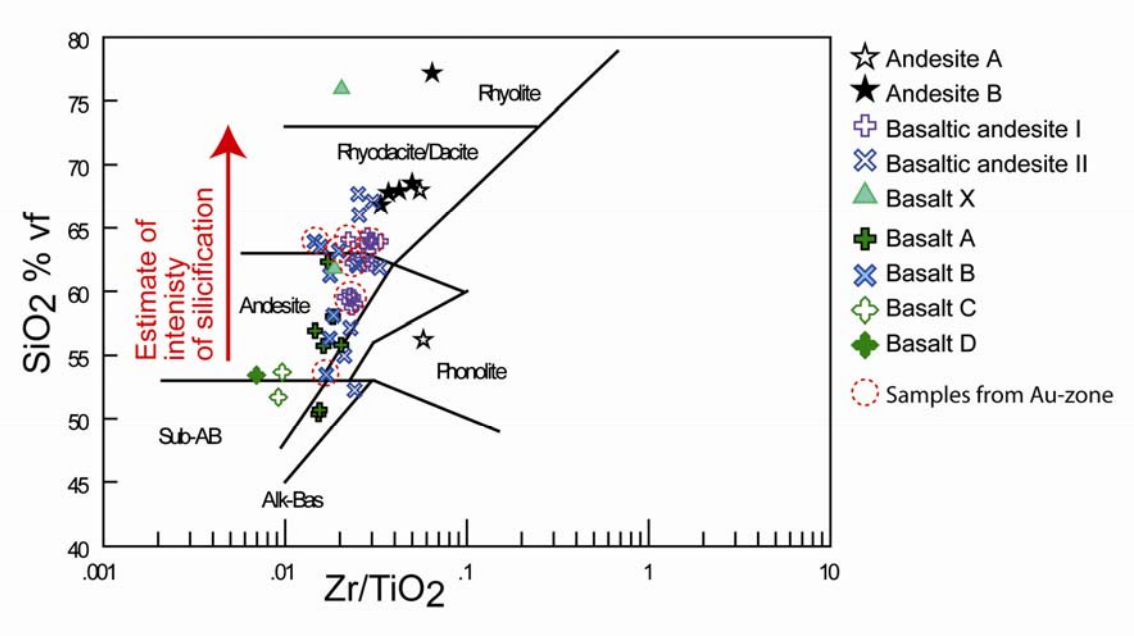

Figure 24. *The diagram based on SiO_2 and Zr/TiO_2 (Winchester and Floyd, 1977) is used to estimate the effects of silicification. It has been shown that the primary rock type of the Qussuk rocks are mafic to intermediate. Many of the Qussuk rocks plot into the fields of felsic rocks (rhyodacite, dacite and rhyolite) which can be explained by silicification. The rocks from the Au-zone are not more intensely silicified than the rocks from outside the gold zone. (vf = volatile free basis).*

Samples which yield a primary basaltic or andesitic composition plot in the fields of andesites and rhyodacite/dacite to rhyolite (Fig. 24). This is in agreement with the observation of silicification of rocks of the Au-zone. Interestingly, the rocks from the Au-zone are not the most silicified rocks, which suggests that either the most silicified rocks represent the distal alteration zone of the Au-mineralisation or that some rocks were altered at an earlier stage. It is also conceivable that two successive alteration stages had overprinting effects. Similar conclusions can be drawn from figures 23b and 23c, which show that samples from the Au-zone are equally altered than samples from outside the Au-zone. In other words, the samples from the Au-zone are not forming more distinct alteration lines, than the samples not belonging to the Au-zone. It is suggested that relatively large areas were hydrothermally altered and possibly represent distal alteration zones to the Au-mineralisation. Alternatively, this wide alteration halo is not related to the introduction of gold in the ppm range and may be much older. It has been seen elsewhere that different alteration and mineralisation styles of different ages can occur within the same district (Yeats and Groves 1998).

The alteration halo at Swan N is about 20 to 25 m wide, comprises up to 3 horizons, each about 1 m thick with gold contents > 1 ppm and the outer and inner alteration zones are generally elevated in gold above 100 ppb (Appendix A).

At Plateau the alteration halo around the gold mineralisation comprising inner and outer alteration zone is narrower and extends a few meters on both sides of the quartz vein with VG. Simi-

lar to the Swan N area, this alteration halo shows elevated gold contents up to several 100 ppb (Appendix A).
The locus of the alteration zones at Swan N and Plateau is structurally controlled because gold quartz veins are located within shear zones, which in turn are close to or at lithological contacts.
The understanding of the hydrothermal alteration process in the Qussuk area can be advanced by quantifying the different alteration styles. However, the limited amount of samples and particularly too few least altered rock samples in the data set makes it difficult to carry out advanced alteration studies at this stage.
Earlier investigations concluded that the gold mineralisation at Qussuk relates to epithermal or VMS type alteration and that the gold mineralisation belongs to the "epithermal clan" (Andreasen 2007; Garde 2008). It was, however, shown in this study that gold is hosted in a quartz vein system within shear zones together with biotite-muscovite-quartz-sulphide-Au alteration and that the base metal content of the rocks is always low. This, together with a gold halo in the ppb range are typical characteristics for orogenic gold deposits (e.g. Groves et al. 2003). Garde (2007) suggested that the rocks of the Qussuk area were formed in an volcanic arc setting and such setting is particularly favourable to host orogenic gold deposits (Fig 25, e.g. Groves et al. 2003).

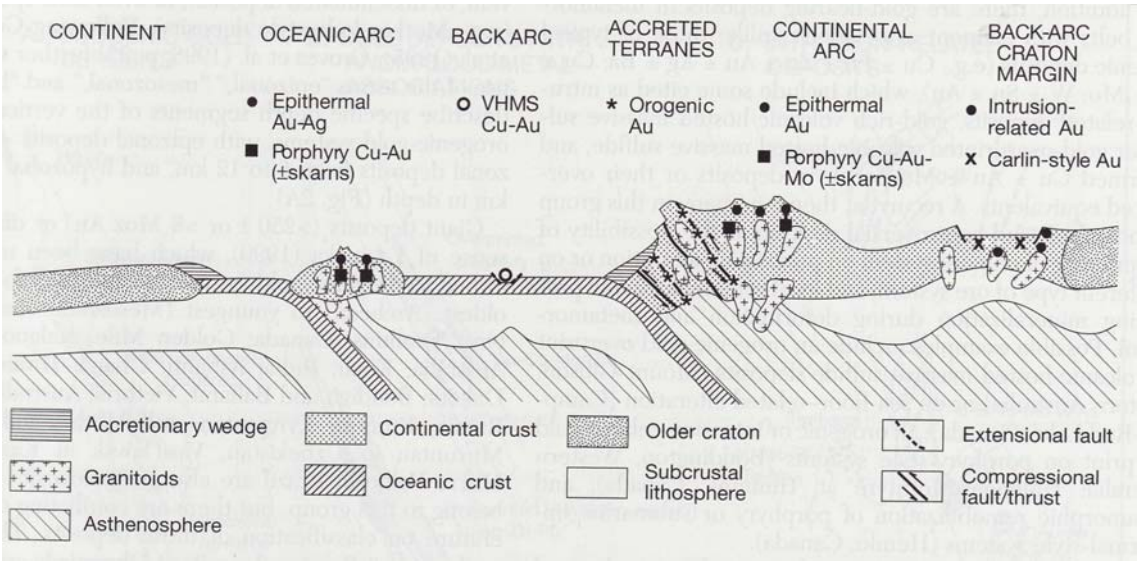

Figure 25. *Tectonic setting of gold deposits, from Groves (2003). Qussuk rocks are suggested to be part of an relict arc complex (Garde, 2007) and from figure 25 it can be seen that arc settings are favourable for Au deposits.*

The gold at Qussuk and the gold at Storø (Eilu et al. 2006, Knudsen et al. 2007) are both hosted in a quartz vein system and both targets are spatially associated with the Ivinnguit fault.
The mineralised Qussuk structure is about 10 to 20 km away from the Ivinnguit fault (Fig. 1) and may represent a second- or third-order structure, which has been shown to be favourable sites for orogenic gold deposits (Eilu and Groves 2001).
The quartz veins with VG and the inner pyrrhotite alteration zone are slightly oblique to the main foliation, therefore it is conceivable that the gold at Plateau is of epigenetic origin. Metamorphic minerals of slightly lower metamorphic grade replacing minerals of higher metamorphic grade indicate that retrograde greenschist metamorphism took place.
At Storø the host rocks yielded an age of 2.8 Ga and the age of the Au-mineralisation yielded 2.63 Ga (Nutman et al. 2007; Van Gool et al. 2007). The time span between 2.6 and 2.7 Ga represents a favourable time period, where globally many million ounces of orogenic gold has been produced e.g. in Yilgarn, Australia and Superior in Canada (Figure 3 in Groves et al. 2003). In the Nuuk area, similar mineralisation ages were determined (Van Gool et al. 2007) and, therefore, it represents a good target area for future gold exploration in southern West Greenland.

Recommendations for further work

- Establishing of additional geological drill profiles from the Swan N and from the Plateau area along strike in order to assess if the Au-zone can be correlated; and to verify if the Au-zone occurs always at the same lithological contact.
- Geological drill profiles should be carried out from the Swan area
- Favourable units at Qussuk should be located by identifying basaltic andesite I in the additional drill profiles. This can be easily carried out directly from the drill cores by using a handheld XRF instrument.
- Structural mapping of the Qussuk area and detailed mapping of the shear zones, in order to identify the gold mineralised shear zones and the quartz vein systems.
- Additional sampling of least altered rocks of each rock type would allow to quantify the effects of alteration (mass change calculations)
- A quartz-sillimanite-fuchsite rock from Ivisaat mountain (Fig 13b) containing monazite was dated by Garde (2008) and reveals an age of 2985 Ma. This age was interpreted by the author as a metamorphic age. The age of the Qussuk mineralisation potentially can be determined from allanite seen in the Au-zone of Plateau (BH 14 at 36.7 m, figure 12). Garnet-rich rocks from the structural hanging wall at Plateau contain abundant monazite and hence can be dated (BH 02 at 13.95, figure 11b). These additional age determinations from Qussuk will provide new information and help to further classify the Qussuk gold mineralisation.
- Garnet-biotite thermometry in order to determine precisely the PT-conditions of gold mineralisation and hydrothermal alteration.
- A similar study (as the one presented here) is suggested to be carried out at Storø which should include detailed drill core logging and sampling in order to accurately establish the geological setting and the chemostratigraphy of the host rocks. Such a study would also allow the comparison of the Storø area with the Qussuk area and other areas which host gold mineralisation (e.g. Qilanngaarsuit).

Acknowledgements

The GEUS report 2010/10 "Geological, petrographical and lithogeochemical investigations on the Qussuk gold mineralisation, southern West Greenland" is published with the permission of director Ole Christiansen from NunaMinerals, Nuuk.

NunaMinerals is thanked for financial support.

Mr. Christiansen is thanked for giving us the permission to make the results of this study available to other interested parties, and he is also thanked for inspiring discussions and his interest in this study. From the NunaMinerals office Nuuna Papis is particularly thanked, but also the rest of the staff is thanked for having fixed all the logistical aspects for the work carried out in Greenland.
Alfons Berger from the Geological Institute in Copenhagen is thanked for his help with the analyses and interpretation of the microprobe data and Nynke Keulen from GEUS is acknowledged for her help with the SEM.
Jochen Kolb, Bo Møller Stensgaard, Adam Garde and Pasi Eilu are thanked for interesting discussions and Jochen Kolb is particularly thanked for his help with petrographic microscopy and having reviewed an earlier version of this report. His comprehensive and detailed review has substantially improved the report.

References

Andreasen B (2007) Mineralogical and geochemical investigations of gold-bearing Mesoarchaean supracrustal rocks from the Qussuk area, southern West Greenland, Mineral resource assessement of the Archean Craton (66º to 63º30'N) SW Greenland, Contribution no.6 Danmarks og Grønlands Geologiske Undersøgelse Rapport 2007/79, 77 pp + 1 CD.

Appel PWU, Coller D, Vincent C, Heijlen W, Moberg ED, Polat A, Raith J, Schjøth F, Stendal H, Thomassen B (2005) Is there a gold province in the Nuuk region? Report from field work carried out in 2004. Danmarks og Grønlands Geologiske Undersøgelse Rapport 2005/27, 79 pp. + 1CD-Rom.

Barrett TJ, MacLean WH (1994) Chemostratigraphy and hydrothermal alteration in exploration for VHMS deposits in greenstones and younger volcanic rocks. In: Lentz DR (ed) Alteration and alteration processes associated with ore-forming systems. Short Course Notes, Volume 11. Geological Association of Canada, pp 433-467.

Christensen R (2007) Prospecting in the Qussuk area. 2006. Unpublished report for Nunaminerals 15 pages and 4 appendices.

Christensen R (2008) Prospecting in the Qussuk area. 2007. Unpublished report for Nunaminerals 22 pages and 4 appendices.

Christensen R (2010) Prospecting in the Qussuk area. 2009. Unpublished report for Nunaminerals, in preparation.

Eilu P, Groves DI (2001) Primary alteration and geochemical dispersion haloes of Archaean orogenic gold deposits in the Yilgarn Craton: the pre-weathering scenario. Geochemistry: Exploration, Environment, Analysis 1: 183-200.

Eilu P, Garofalo P, Appel PWU, Heijlen W (2006) Alteration patterns in Au-mineralised zones of Storø, Nuuk region - West Greenland. Danmarks og Grønlands Geologiske Undersøgelse Rapport 2006/30, 73 pp.

Escher JC, Pulvertaft TCR (1995) Geological map of Greenland, 1:2 5000 000. Copenhagen: Geological Survey of Greenland.

Evensen NM, Hamilton PJ, O'Nions RK (1978) Rare-earth abundances in chondritic meteorites. Geochimica et Cosmochimica Acta 42: 1199-1212

Galley AG, Koski RA (2000) Setting and characteristics of ophiolite-hosted volcanogenic massive sulphide, deposits. Rev. Econ. Geol., v8: 221-246.

Garde AA (1988) Geological map of Greenland, 1:100 000. Copenhagen: Geological Survey of Greenland.

Garde AA (1997) The Accretion and evolution of an Archaean high-grade grey gneiss - amphibolite complex: the Fiskefjord area, southern West Greenland. Geology of Greenland Survey Bulletin, 177; 115 pages.

Garde AA (2007) A mid-Archaean island arc complex in the eastern Akia terrane, Godthåbsfjord, southern West Greenland. Journal of the Geological Society, London 164: 565-579.

Garde AA (2008) Geochemistry of Mesoarchaean andesite rocks with epithermal gold mineralization at Qussuk and Bjørneøen, southern West Greenland, Mineral resource assessement of the Archean Craton (66º to 63º30'N) SW Greenland, Contribution no.8 Danmarks og Grønlands Geologiske Undersøgelse Rapport 2008/4, 52 pp.

Garde AA, Stendal H, Møller Stensgaard B (2007) Pre-metamorphic hydrothermal alteration with gold in a mid-Archaean island arc, Godthåbsfjord, West Greenland. Geological Survey of Denmark and Greenland Bulletin 13: 37-40.

Groves DI, Goldfarb RJ, Robert F, Hart CJR (2003) Gold Deposits in Metamorphic Belts: Overview of Current Understanding, Outstanding Problems, Future Research, and Exploration Significance. Economic Geology 98: 1-29.

Hollis JA, Schmid S, Stendal H, van Gool JAM, Lehmann Weng W (2006) Supracrustal belts in Godthåbsfjord region, southern West Greenland. Progress report on 2005 field work: geological mapping, regional hydrothermal alteration and tectonic sections. Danmarks og Grønlands Geologiske Undersøgelse Rapport 2006/7, 171 pp. + 1 DVD.

Hollis JA, van Gool JAM, Steenfelt A, Garde AA (2004) Greenstone belts in the central Godthåbsfjord region, southern West Greenland: preliminary results from field work in 2004. Danmarks og Grønlands Geologiske Undersøgelse Rapport 2004/110, 110 pp. + 1 DVD.

Hollis JA, van Gool JAM, Steenfelt A, Garde AA (2005) Greenstone belts in the central Godthåbsfjord region, southern West Greenland. Geological Survey of Denmark and Greenland Bulletin 7: 65-68.

Knudsen C, van Gool JAM, Østergaard C, Hollis JA, Rink-Jørgensen M, Persson M, Szilas K (2007) Gold-hosting supracrustal rocks on Storø, southern West Greenland: lithologies and geological environment. Geological Survey of Denmark and Greenland Bulletin 13: 41-44.

Kolb J, Møller Stensgaard B, Schlatter D, Dziggel A (2009) Controls of hydrothermal quartz vein mineralisation and wall rock alteration between Ameralik and Sermilik, southern West Greenland, Danmarks og Grønlands Geologiske Undersøgelse Rapport 2009/25, 76 pp. + 1 DVD.

Le Bas MJ, Le Maitre RW, Streckeisen A, Zanettin B (1986) A chemical classification of volcanic rocks based on the total alkali-silica diagram. Journal of Petrology 27: 745-750.

MacLean WH, Barrett TJ (1993) Lithogeochemical techniques using immobile elements. Journal of Geochemical Exploration 48: 109-133.

McPhie J, Doyle M, Allen R (1993) Volcanic textures. A guide to the interpretation of textures in volcanic rocks. Hobart, University of Tasmania, Centre for Ore Deposit and Exploration Studies, 196 pages.

NunaMinerals (2008a) NunaMinerals A/S, Årsrapport 2007 (yearly company report 2007), pp 35.

NunaMinerals (2008b) Qussuk guld-kobber-projekt, Resultater 2007, Press Release, 4.02.2008.

NunaMinerals (2008c) Resultater fra 2007 bekræfter den positive udvikling af Storø guldprojektet, Press Release, 30.01.2008.

Nutman AP, Christiansen O, Friend CRL (2007) 2635 Ma amphibolite facies gold mineralisation near a terrane boundary (suture?) on Storø, Nuuk region, southern West Greenland. Precambrian Research 159: 19-32.

Pearce JA (1996). A user's guide to basalt discrimination diagrams. In: Wyman DA (ed) Trace element geochemistry of volcanic rocks: applications for massive sulphide exploration. Geological Association of Canada. Short Course Notes, Vol. 12: 79–113.

Poulsen KH, Hannington MD (1995) Volcanic-associated massive sulphide gold. In: Eckstrand OR, Sinclair WD, Thorpe RI (eds) Geology of Canadian mineral deposit types. Geological Society of America, DNAG. Geology of Canada, no. 9. Geological Survey of Canada, Canada, pp 183-196.

Schlatter DM (2007) Volcanic Stratigraphy and Hydrothermal Alteration of the Petiknäs South Zn-Pb-Cu-Au-Ag Volcanic-hosted Massive Sulfide Deposit, Sweden, Ph.D. thesis, Department of Chemical Engineering and Geosciences, Division of Ore Geology and Applied Geophysics. Luleå University of Technology, ISSN: 1402-1544, 193 pages.

Schlatter DM, Christensen R (2010) Geological, petrographical and geochemical investigations on the Qussuk gold mineralization, southern West Greenland. In: Nakrem HA, Harstad AO, Haukdal G (eds) 29th Nordic Geological Winter Meeting, Geological Society of Norway, p 173.

Smith GM (1998) Geology and mineral potential of the Bjørnøen supracrustal belt, Nuukfjord, West Greenland. Unpublished report, Nunaoil A/S, 13 pp. (in achives of Geological Survey of Denmark and Greenland, GEUS Report File 21649).

Stendal H (2007) Characterisation of selected geological environments. Mineral resource assessement of the Archean Craton (66º to 63º30'N) SW Greenland, Contribution no.1 Danmarks og Grønlands Geologiske Undersøgelse Rapport 2007/20, 90 pp.

Stensgaard Møller B (2008) Gold favourability in the Nuuk region, southern West Greenland: results from fieldwork follow-up on multivariate statistical analysis. Mineral resource assessment of the Archaean Craton (66° to 63°30´N), SW Greenland. Contribution no. 9.Danmarks og Grønlands Geologiske Undersøgelse Rapport 2008/08, 74 pp.

Sun S, McDonough WF (1989) Chemical and isotopic systematics of oceanic basalts: implication for mantle composition and processes. In: Saunders AD, Norry MJ (eds.) Magmatism in the Ocean basins. Geol. Soc. London, Spec. Publ. 42: 313–345

Yeats CJ, Groves DI (1998) The Archaean Mount Gibson gold deposits, Yilgarn Craton, Western Australia: Products of combined synvolcanic and syntectonic alteration and mineralisation. Ore Geology Reviews 13: 103-129.

Van Gool JAM, Scherstén A, Østergaard C, Neraa T (2007): Geological setting of the Storø gold prospect, Godthåbsfjord region, southern West Greenland. Result of detailed mapping, structural analysis, geochronology and geochemistry. Danmarks og Grønlands Geologiske Undersøgelse Rapport 2007/83 , 158 pp.

Winchester JA, Floyd PA (1977) Geochemical discrimination of different magma series and their differentiation products using immobile elements. Chemical Geology 20: 325-343.

Østergaard C, van Gool JAM (2007) Assessment of the gold mineralisation on Storø, Godthåbsfjord, southern West Greenland. Mineral resource assessement of the Archean Craton (66º to 63º30'N) SW Greenland, Contribution no.5. Danmarks og Grønlands Geologiske Undersøgelse Rapport 2007/78, 20 pp.

List of Appendices on CD-Rom:

Appendix A: NunaMinerals Qussuk drilling 2008 and 2009: simplified results of drill core analyses.
Appendix B: Electronic field book: GanFeld data from digital field data capture system (GSC and further developed by GEUS).
Appendix C: Detailed geological drill core logging of 4 bore holes from the Swan N and Plateau areas.
Appendix D: EMPA data from Geological Institute in Copenhagen (JEOL JXA-8200 superprobe).
Appendix D extra: microphotographs of probed spots; BSE images from superprobe.
Appendix E: SEM data from GEUS (PHILIPS XL 40 SEM).
Appendix F: Geochemical data compiled (on a volatile free basis) and gold.
Appendix G-1: Compiled geochemical raw data and gold as reported by Actlabs.
Appendix G-2: Gold and a few traces; raw data as reported by Actlabs.
Appendix H: Chemical classification of all the samples of this study.